Metal Ion Detection by Luminescent Metal Organic Frameworks

by

Peyman Sirous

A Thesis Presented in Partial Fulfillment
of the Requirements for the Degree
Master of Science

Approved April 2018 by the
Graduate Supervisory Committee:

Bin Mu, Co-Chair
Terry Alford, Co-Chair
Yang Jiao

ARIZONA STATE UNIVERSITY

May 2018

ABSTRACT

Metal Organic Frameworks(MOFs) have been used in various applications, including sensors. The unique crystalline structure of MOFs in addition to controllability of their pore size and their intake selectivity makes them a promising method of detection. Detection of metal ions in water using a binary mixture of luminescent MOFs has been reported. 3 MOFs(ZrPDA, UiO-66 and UiO-66-NH$_2$) as detectors and 4 metal ions(Pb^{2+}, Ni^{2+}, Ba^{2+} and Cu^{2+}) as the target species were chosen based on cost, water stability, application and end goals.

It is possible to detect metal ions such as Pb^{2+} at concentrations at low as 0.005 molar using MOFs. Also, based on the luminescence responses, a method of distinguishing between similar metal ions has been proposed. It is shown that using a mixture of MOFs with different reaction to metal ions can lead to unique and specific 3D luminescence maps, which can be used to identify the present metal ions in water and their amount.

In addition to the response of a single MOF to addition of a single metal ion, luminescence response of ZrPDA + UiO-66 mixture to increasing concentration of each of 4 metal ions was studied, and summarized. A new peak is observed in the mixture, that did not exist before, and it is proposed that this peak requires metal ions to activate.

ACKNOWLEDGMENTS

First, I would like to thank my co-chairs, Profs. Mu and Alford, for all their help and guidance during my studies. I have learned a lot, and hopefully with their support I will continue to improve myself.

Second, Mitch, Bohan and Sean who taught me everything in the lab, and helped me whenever something went wrong.

Next, I want to thank my girlfriend Melika. Coming to the US was a huge risk, and it required a lot of effort and sacrifice. I would have never been able to make it without you.

Mom and dad, with your support, I was able to follow my dreams and grow, to the best of my capabilities. You always had my back, and always made me feel secure.

Ashkan, Saman and Elham, even though you are not here with me, you are my family, and will always be in my mind.

And last, I want to thank Dr. Darrel Frear. While we worked with each other for a short amount of time, you showed so much support and care, and it restored my faith in people. I will never forget how much you helped me.

TABLE OF CONTENTS

LIST OF TABLES

LIST OF FIGURES

Figure

Page

Chapter 1

INTRODUCTION

1.1   Introduction to MOFs

Metal Organic Frameworks (MOFs) are an emerging class of crystalline materials that are gaining more attraction in recent years due to their unique properties such as high surface area, nano-pores and luminescent properties. There are many different MOFs that can be made using different metals such as Zr, Zn, Cu and rare earth metals such as La and Eu, and based on the ligands used, many of the properties such as pore size, crystallinity, luminescence etc. can be controlled.

MOFs have been widely studied for their use in catalysis, drug delivery, gas separation, gas storage and sensors. The small pore size allows certain molecules to enter, and limits access to some others, which increases the selectivity of reactions when the MOF is used as a catalyst. The small pores can also act as a storage area for gasses or in drug delivery, and they can release the compounds in side when a certain change in environment happens. For sensors, due to their luminescent properties, they can detect different metal ions and solvents, and recently there has been some research on detecting nerve gas agents. Armstrong *et al.* (2017); Fang *et al.* (2006); Murray *et al.* (2009)

1.2   Introduction of MOFs used in this project

1.2.1   UiO-66

University of Oslo (UiO) are a series of MOFs that due to their high stability and surface area, have attracted a lot of attention. UiO-66 is one of the most stable

MOFs that has been reported to this date, showing stability in contact with many solvents such as water, and thermal stability to 500 C. As can be seen in Figure 1.1, UiO-66 has a Cubic Close Packed(CCP) structure. Cavka *et al.* (2008)
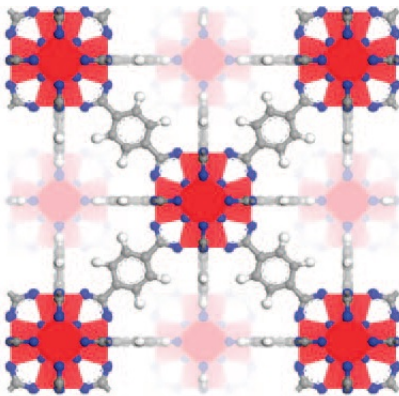
Figure 1.1: UiO-66 in which Zirconium atoms are red, Oxygen is blue, Carbon is grey and Hydrogen is white. Cavka *et al.* (2008)

Due to the 7.5(Å) triangular pores in UiO-66, metal ions can easily enter the pores Chavan *et al.* (2012). This property, together with water stability and strong luminescent properties makes UiO-66 a good candidate for detection of metal ions in water.

1.2.2   UiO-66-NH$_2$

UiO-66-X MOFs were a series of MOFs that were based on the same structure and topology of UiO-66, but pore functionality and size were changed through a change in ligand. Figure 1.2 shows H$_2$N-H$_2$BDC linker. Kandiah *et al.* (2010a)

The Langmuir experimental surface area of UiO-66-NH$_2$ ($\sim$ 1250 m^2/g) is not that different from UiO-66($\sim$ 1300 m2/g), while the pore size for UiO-66-NH$_2$ is around 6(Å) Kandiah *et al.* (2010a); Song *et al.* (2017). Figure 1.3 shows a side by side comparison of UiO-66 and UiO-66-NH2.
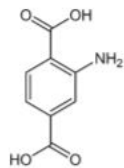
Figure 1.2: H₂N H₂BDC linker used for synthesizing UiO-66-NH₂.
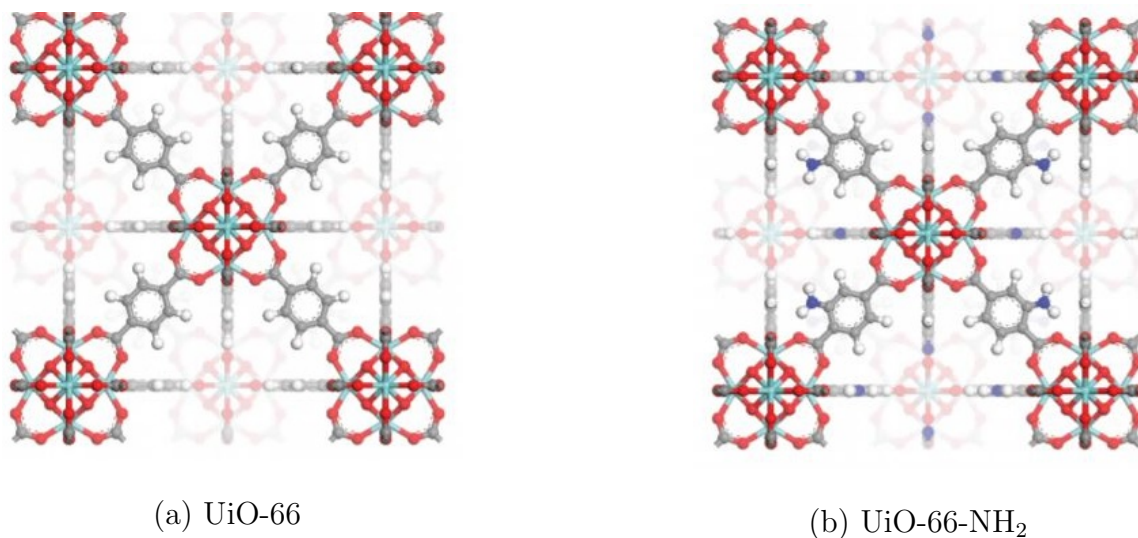
(a) UiO-66

(b) UiO-66-NH₂

Figure 1.3: Side by side comparison of the structure of (a) UiO-66 and (b) UiO-66-NH₂. Carbon atoms are shown in gray, Hydrogen is white, Oxygen is red, Zirconium is cyan and Nitrogen is blue

1.2.3 ZrPDA

One recent research area for possible MOF application is usage of MOFs as a semiconductor. There has been some research done on band gap tuning based on variations in the ligand, but most of the research is focused on changes before synthesis. Lin *et al.* (2012); Flage-Larsen and Thorshaug (2014)

As an alternative, ZrPDA was designed. In ZrPDA, it is possible to tune the band-gap using an external catalyst such as light. It is also moisture and water stable, which makes it suitable for uses in water. Mu and Shan (2017)

3

While there has not been any research on luminescent properties of ZrPDA, water stability, strong photo-emission, and the fact that it also uses Zirconium ions as the metal node makes ZrPDA a very suitable MOF for this project. Figure 1.4 shows 1,4-phenylenediacrylic acid linkers used in ZrPDA synthesis. The main luminescence mode of ZrPDA has not been determined yet, but due to the two C=C bonds in the ligand, it is possible that electron delocalization may be stronger, and the main luminescence mode may be LMCT.
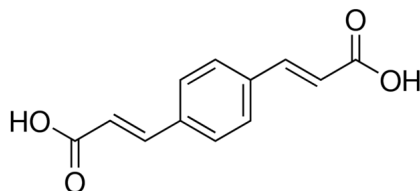
Figure 1.4: chemical structure of 1,4-phenylenediacrylic acid linkers used in ZrPDA synthesis

1.3 Synthesis of the MOFs

The synthesis method used for all the MOFs in this project is solvothermal synthesis. Solvothermal synthesis is one of the most important synthesis methods which is frequently used in MOF synthesis. Normally, the reactants are dissolved in a solvent, mixed in a Teflon-lined stainless-steel reactor or in glass tubes, and then kept at 100-200C for 12-24 hours. There are examples of longer reaction time or lower temperatures in the literature such as $Zn_3O(BTC)_2(DMF)$ reported by Fang *et al.* (2006), but the majority of MOFs are synthesized under the aforementioned conditions.

In solvothermal synthesis, the reaction will occur as the temperature increases, which will dissolve any reactant that has was not dissolved at room temperature, and will also increase the pressure inside the reactor. This method is cheap, easy to use

and can be used to create a lot of the common MOFs such as UiO-66 and ZnBTC.

1.4 Luminescence in MOFs

Luminescence in MOFs is a field that has attracted a lot of attention due to the hybrid nature of MOFs, which enables a wide range of emissions and emission sources. The term luminescence is used to encompass different types of emission such as fluorescence, phosphorescence and scintillation. Allendorf *et al.* (2009)

Because of the unique structure of MOFs, there can be many sources for luminescence, but the main ones include:

- Linker-based luminescence, including ligand-localized emission as well as ligand-to-metal charge transfer (LMCT) and metal-to-ligand charge transfer (MLCT).

- Metal-based emission.

- Antennae effects.

- Adsorbate-based emission and sensitization.

- Excimer and exciplex emission

- Surface functionalization

- Scintillation

Since many MOFs have permanent pores, guest molecules, atoms or ions can be absorbed and held next to the luminescence centers. These guests can change the emission via a change in wave length, intensity or addition of new emissions via excimer or exciplex formation. Also, since MOFs retain their structures, their surface and sites can be functionalized. The combination of these properties and possibilities

makes MOFs very attractive for applications such as small molecule sensors. Allendorf *et al.* (2009)

There are 5 main mods of luminescence in MOFs: linker based, metal ion based, adsorbed lumophore entity, bonded surface lumophore and exciplex formation. Terephthalic acid which is used in UiO-66 and 2-aminoterephthalic acid used in UiO-66-NH2 has been shown to have linker based, Linker to Metal Charge Transfer(LMCT) luminescence mode. Wei Chen *et al.* (2003); Zhang *et al.* (2007)

The luminescence mode of 1,4-phenylenediacrylic acid has not been studied yet, and but for similar ligands such as 1,4-Phenylenediacetic acid, it has been shown that LMCT and $\pi^* \to \pi$ transition of intraligand(IL) can be detected. Liu *et al.* (2009); Yang *et al.* (2010); Braverman and LaDuca (2007)

It is also important to keep in mind that different modes of luminescence can be present in the MOF, and they can also be activated at the same time. Each of these luminescence modes has their own excitation and emission wavelength, and they also behave differently when environmental conditions change. Sometimes stronger emission modes can overshadow a peak originating from another mode, creating a false image that the only active mode is the predominant one. Cui *et al.* (2012)

Since it is believed that LMCT is the predominant mode of luminescence for the MOFs used in this project, the focus will be on introducing LMCT. The effects that other modes can have on the intensity of the luminescence peak has been accepted as a small error.

LMCT involves a transfer from a localized orbital of the linker to the orbitals of the metal node. LMCT is usually reported in structures containing derivatives of benzene. LMCT emissions can be in different wavelengths, from intense emissions of [Zn(2,3-pydc)(bpp)] . 2.5H2O (2,3-pydcH$_2$ = pyridine-2,3-dicarboxylic acid) at 436 nm Wang *et al.* (2009), to strong yellow emissions of Cu$_5$(SCN)$_5$(3-Abpt)$_2$ (3-

Abpt=4-amine-3,5-bis(3-pyridyl)-1,2,4-triazole). Li *et al.* (2009)

Although sometimes LMCT luminescence may compete with ligand-based luminescence, the intense luminescence peaks and the diversity of excitation and emission wavelengths in MOFs with LMCT emission makes them a suitable choice for many applications such as sensors and detectors. Cui *et al.* (2012)

There has been a lot of research on using luminescent MOFs as a detector or sensor for various applications and environments. Uses such as detecting explosives Kim *et al.* (2013), ammonia Shustova *et al.* (2013), gunshot residue Weber *et al.* (2011), temperature Rao *et al.* (2013) and many papers on detecting small molecules and ions. Chen *et al.* (2007, 2008); Luo and Batten (2010)

Chapter 2

SYNTHESIS, CHARACTERIZATION, TESTING METHODS AND RESULTS

2.1 Introduction

While there has been a lot of research on using MOFs to detect metal ions, one of the main limitations that this method is facing is distinguishing between different metal ions. Certain MOFs are very sensitive to one ion, but show moderate to no sensitivity to other ions. For example, when using $Eu_2(FMA)_2(OX)(H_2O)_4.4H_2O$, luminescence intensity of $Cu(NO_3)_2$ is very different from other metal ions, but $Ca(NO_3)_2$, $Mg(NO_3)_2$ and $Cd(NO_3)_2$ show relatively similar luminescence behavior. This behavior can be seen in Figure 2.1.1. Xiao *et al.* (2010)

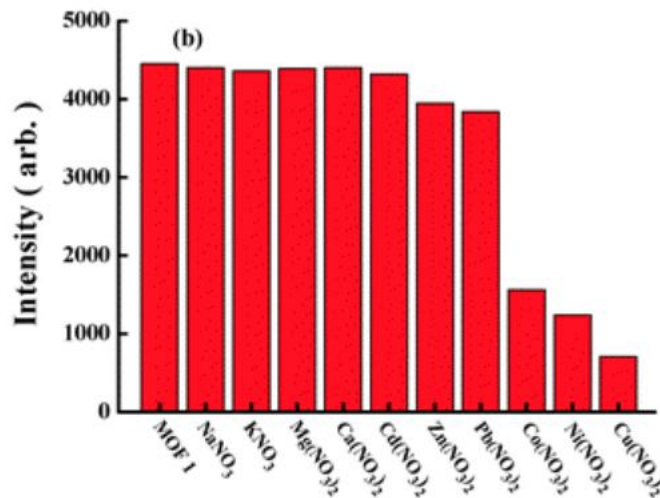Figure 2.1: Luminescence intensity of different metal ions in $Eu_2(FMA)_2(OX)(H_2O)_4.4H_2O$ Xiao *et al.* (2010)

Because of this, the application of luminescent MOFs in metal ion detection can

be very limited. In a lab environment, where the exact concentration of ions is known, it is possible to detect the concentration of the metal ion with acceptable precision, but a mixture of ions can introduce a lot of error into the readings. For example, a mixture of two ions, one with quenching effect, and one with enhancing effect can result in minimal change in luminescence, giving the false conclusion that there are no metal ions present. Since for many applications, the present metal ions are already known, it may be possible to choose a MOF that shows the behavior that we want. But using this method, the uncertainty for the readings can be very high, resulting in a need for complementary techniques to ensure the readings from the MOF detector are accurate.

Another way to combat this drawback, is to use a mixture of MOFs. Since different MOFs show different responses to the same metal ion, it may be possible to conclude what metal ions are present based on the response from more than one MOF. For example, introduction of Lead cations in the solution has close to no effect on the luminescence of ZrPDA, while it has a very strong quenching effect on the luminescence of UiO-66. Using a mixture of ZrPDA and UiO-66 in theory should increase the certainty that the detected metal ion is Lead, and the concentration is accurate.

While there is limited research on using luminescent MOF mixtures as sensors such as using a mixture to detect VOCs Balzer *et al.* (2017), these papers only detect the overall peak change at a certain wavelength. To the best of my knowledge there is no report documenting using a 3D luminescence map of a MOF mixture and detecting the change in the peaks for all the MOFs.

One of the reasons for the lack of research on MOF mixtures is that MOFs can also change the luminescence of each other, making it hard to have a background to compare the results with. This means for each MOF mixture, there is a need to

run a 3D luminescence map test, and it is not possible to only rely on pure MOF background results. This introduces several additional steps to preparing the sensors, and can increase the amount of work required before MOF mixture is ready to be used.

2.2 Methodology

2.2.1 Materials

All of the chemicals were commercially available and were used without further purification. Zirconium(IV) oxychloride octahydrate($\geq$99.5% Sigma-Aldrich), Zirconium(IV) chloride($\geq$99.5% Aldrich), Terephthalic acid(98% Aldrich), 2-Aminoterephthalic acid ($\geq$99% Aldrich) and 1,4-Phenylenediacrylic acid(97% Aldrich), triethylamine (Sigma-Aldrich), N,N-dimethylformamide, DMF (Sigma-Aldrich), Acetic acid($\geq$99.7% Sigma-Aldrich) and Formic acid($\geq$95% Sigma Aldrich) were used to synthesis the MOFs and Nickel(II) nitrate hexahydrate ($\geq$97% Sigma-Aldrich), Copper(II) nitrate trihydrate (>98% Sigma-Aldrich) Barium chloride (99.9% Aldrich) , Lead(II) nitrate(99% Alfa Aesar) and Deionized water (Sigma-Aldrich) were used for luminescence testing.

2.2.2 Synthesis

Synthesis of UiO-66

A solution of Terephthalic acid (1.5 mmol) and $ZrCl_4$ (1.5 mmol) in DMF (24.0 mL) and Formic acid (5.7 mL) were stirred until a clear solution was achieved, and added to a Teflon-lined stainless-steel autoclave, as previously described in the literature. The solution was heated for 24 hours at 120 °C and then filtered in air for 24 hours to obtain white crystals. Kandiah *et al.* (2010b)

Synthesis of UiO-66-NH$_2$

In a modification to UiO-66, a solution of 2-aminoterephthalic acid (0.35 mmol) and ZrCl$_4$ (0.35 mmol) in DMF (6.6 mL) were stirred until a clear solution was achieved, and added to a Teflon-lined stainless-steel autoclave, as previously described in the literature. The solution was heated for 24 hours at 120 °C and then filtered in air for 24 hours to obtain light-yellow crystals.Kandiah *et al.* (2010b)

Synthesis of ZrPDA

For ZrPDA synthesis, a solution of ZrOCl$_2$.8H$_2$O (0.5 mmol) in Formic acid (2.3 ml) and DMF(10 ml) and a solution of 1,4-Phenyldiacrylic acid (0.5 mmol) in triethylamine (0.15 ml) and DMF (17.7 ml) were mixed together until a clear solution was achieved, then added to a Teflon-lined stainless-steel autoclave. The solution was heated at 120 °C for 24 hours and then filtered in air for 24 hours to obtain white crystals.Mu and Shan (2017)

Activation

To ensure the samples did not contain any residual ligands or metal salts, the samples were washed with DMF and acetone several times. Also, samples were heated at 100 °C for 12 in vacuum to activate the samples and empty the pores from any residual solvent.

2.2.3   Characterization Methods

Crystallinity was analyzed using (Panalytical X Pert Pro) with Pixcel detector using Ni-K radiation (=1.5406 Å). To calculate the surface area and pore volume, TriStar II 3020 analyzer (Micromeritics) BET using Barret-Joyner-Halenda (BJH) model was used, while the average pore diameter for the samples were calculated

by density functional theory (DFT) method using the ASAP 2020 analyzers built-in software.

2.2.4 Testing Luminescence

Luminescence data were collected using Horiba Nanolog Luminometer, with a 3 (ml) quartz testing vial. To prepare the solution, metal salts were dissolved in De-Ionized (DI) water, then the dried and activated MOFs were added, and sonicated for 15-20 minutes to ensure water and the ions have diffused in the MOF pores. To ensure maximum diffusion and contact area between water and MOF, the MOFs were mechanically grinded in a mortar and pestle. Since luminescence is time and temperature sensitive, and the MOF structure and the amount of diffusion can all affect the results, the tests were carried on a certain MOF uninterrupted, with varied ion concentration .

For each luminescence test at a certain concentration, samples from at least 3 different MOF batches that were independently synthesized were used. From each MOF batch, at least 3 samples were taken to test the luminescence at that concentration. To ensure that water degradation or sonication were not affecting the luminescence, tests were run after up to 8 hour sonication and 48 hour water contact, which resulted in the conclusion that their effect was minimal. To ensure that temperature was not affecting the luminescence, measures were taken to ensure temperature would remain constant through sonication.

For some systems, MOF luminescence was saturated after a certain concentration of ions, and the tests were not continued afterwards. For others, the tests were carried from 0-0.05 molar at 0.005 molar intervals, and from 0-0.5 molar at 0.05 molar intervals. The tests were also repeated several times to get an average luminescence result with less error.

For mixed MOF systems, first different ratios of two MOFs were added together to get a appropriate mixture. Due to the low peak intensity of UiO-66-NH$_2$, adding it to ZrPDA or UiO-66 did not affect the luminescence as much. To get usable peaks, very high concentrations(in order of $\sim$ 0.1 molar) of metal ions were needed, and since such systems do not occur that often, they were not followed.

For UiO-66+ZrPDA system, first 20 mg of UiO-66 were added to a vial and tested. Then vials containing 20 mg UiO-66 and 4,8,12,16 and 20 mg ZrPDA were tested, and it was deemed that 20 UiO-66:12 ZrPDA is the best system. For mixture system containing metal ions, a solution of 20mg UiO-66:12 mg ZrPDA was created and tested as the control, then solutions containing higher concentrations of metal ions were created, sonicated for 15-20 minutes, and then tested.

2.3   Results and Discussion

The first step was to test a single metal ion and a single MOF. Based on the requirements and the objectives, ZrPDA, UiO-66 and UiO-66-NH$_2$ were chosen with Ni^{2+}, Cu^{2+}, Ba^{2+}, Pb^{2+}. Since the overall results of luminescence is being studied, a 3D-map of luminescence in addition to peak change is required. Figure 2.2 shows the 3D luminescence of ZrPDA with increasing concentrations of Ni(NO$_3$)$_2$, while Figure 2.3 and 2.4 show the luminescence of UiO-66 and UiO-66-NH$_2$ with increasing concentrations of Ni(NO$_3$)$_2$, respectively. It is important to remember that even though all of these MOFs have a luminescence response peak, the position(excitation and emission wavelength) for them is completely different. So far, most of the research done on using MOFs as a sensor focus on the peak intensity change, but since peak position can also be used, 3D luminescence maps have been included. Also, it is important to note that with increasing concentrations of metal ion, it is common to see a peak shift in luminescence map.
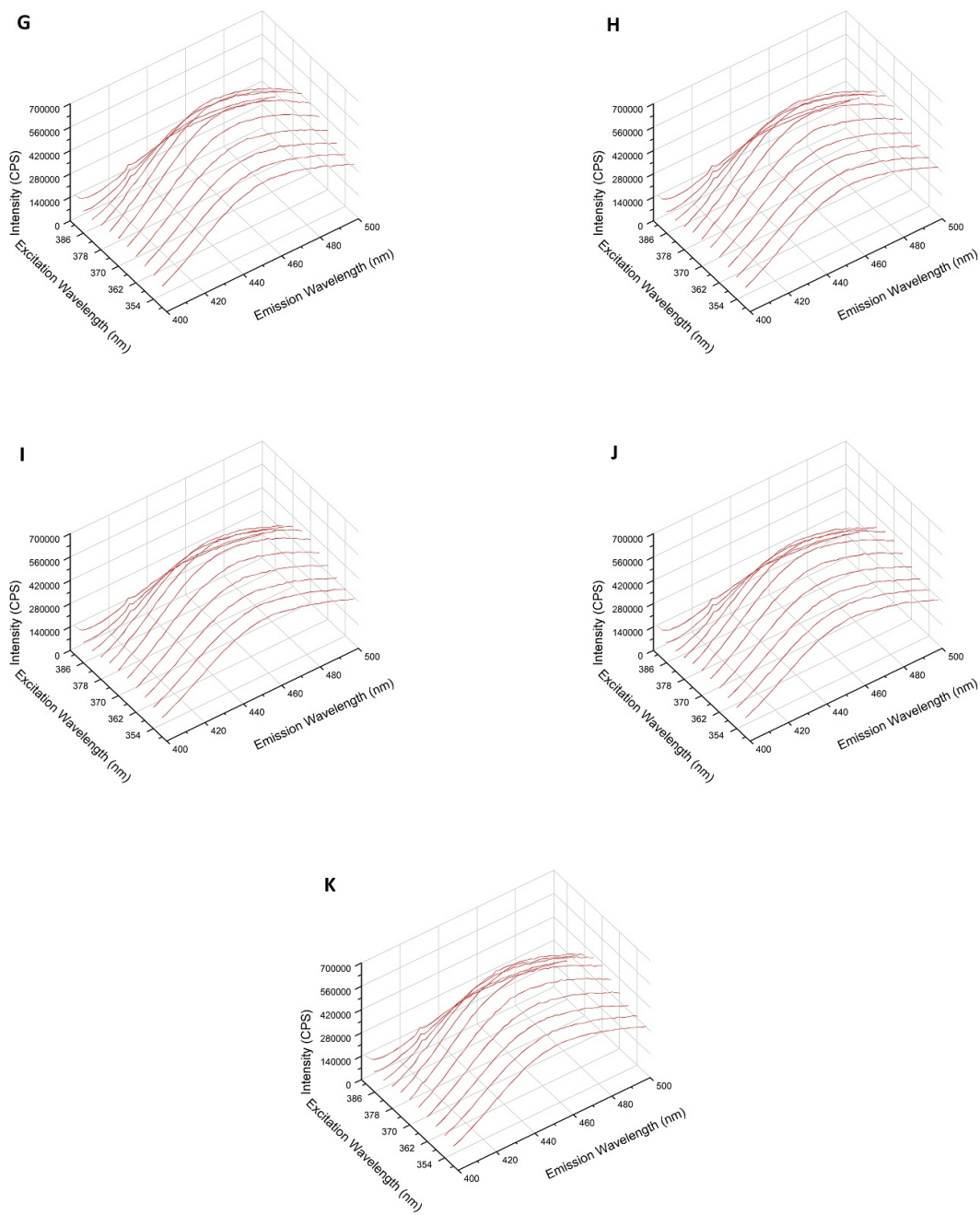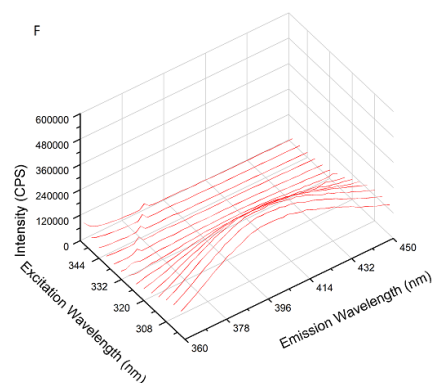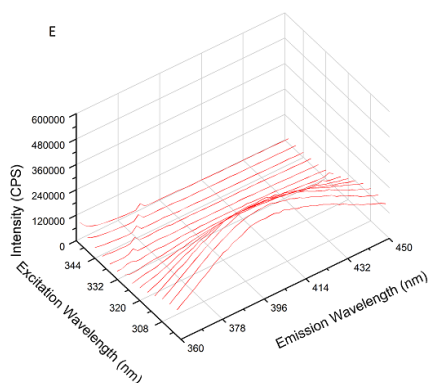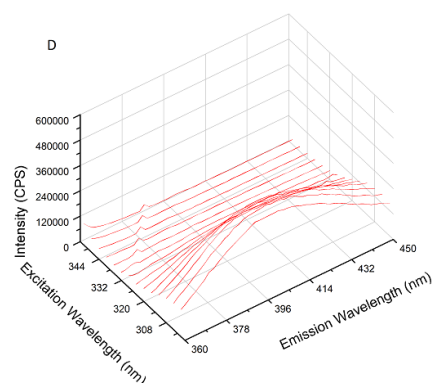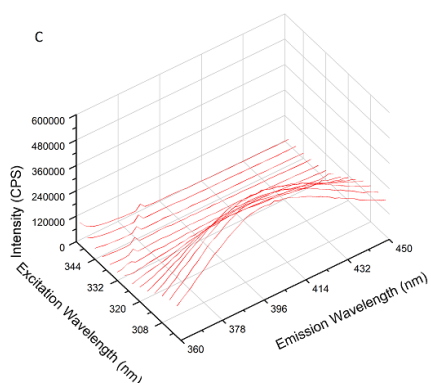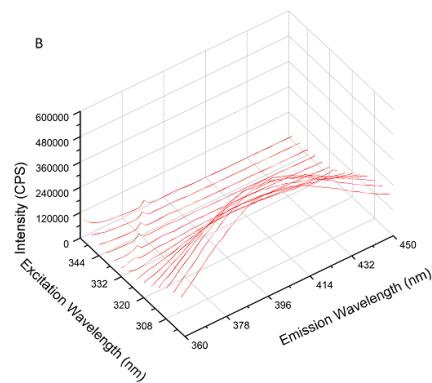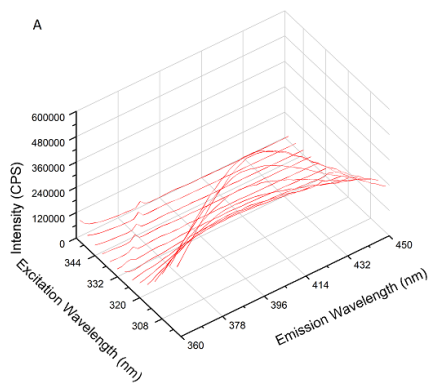
A

B

C

D

E

F

14
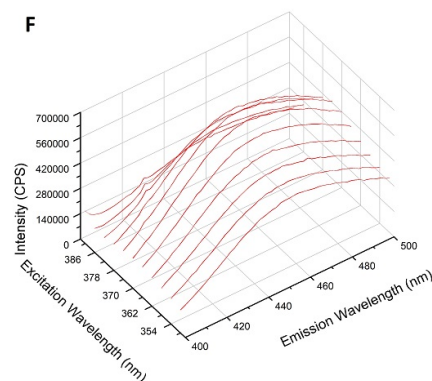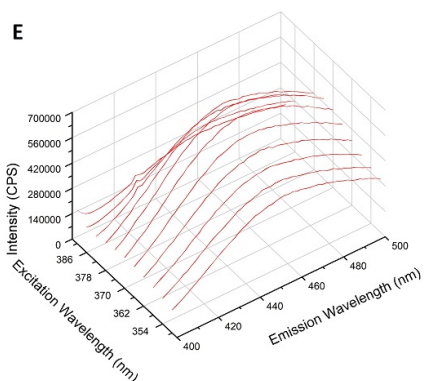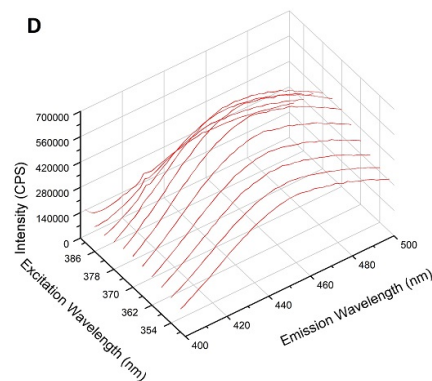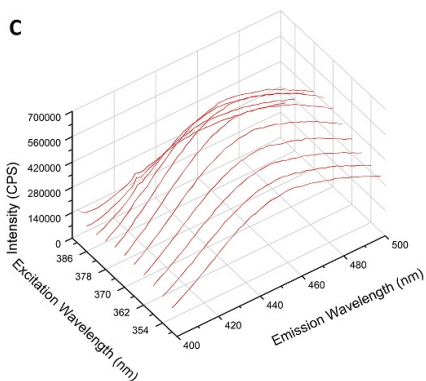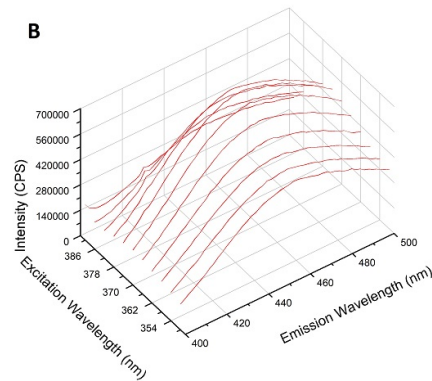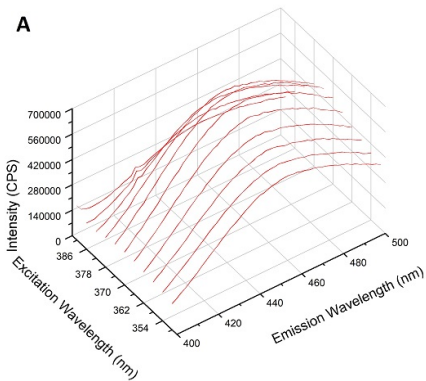
Figure 2.2: 3D luminescence map of (A) pure ZrPDA, (B) 0.005, (C) 0.010, (D) 0.015, (E) 0.020, (F) 0.025,(G) 0.030, (H) 0.035, (I) 0.040, (J) 0.045, (K) 0.050 molar Ni(NO$_3$)$_2$ solution with ZrPDA.
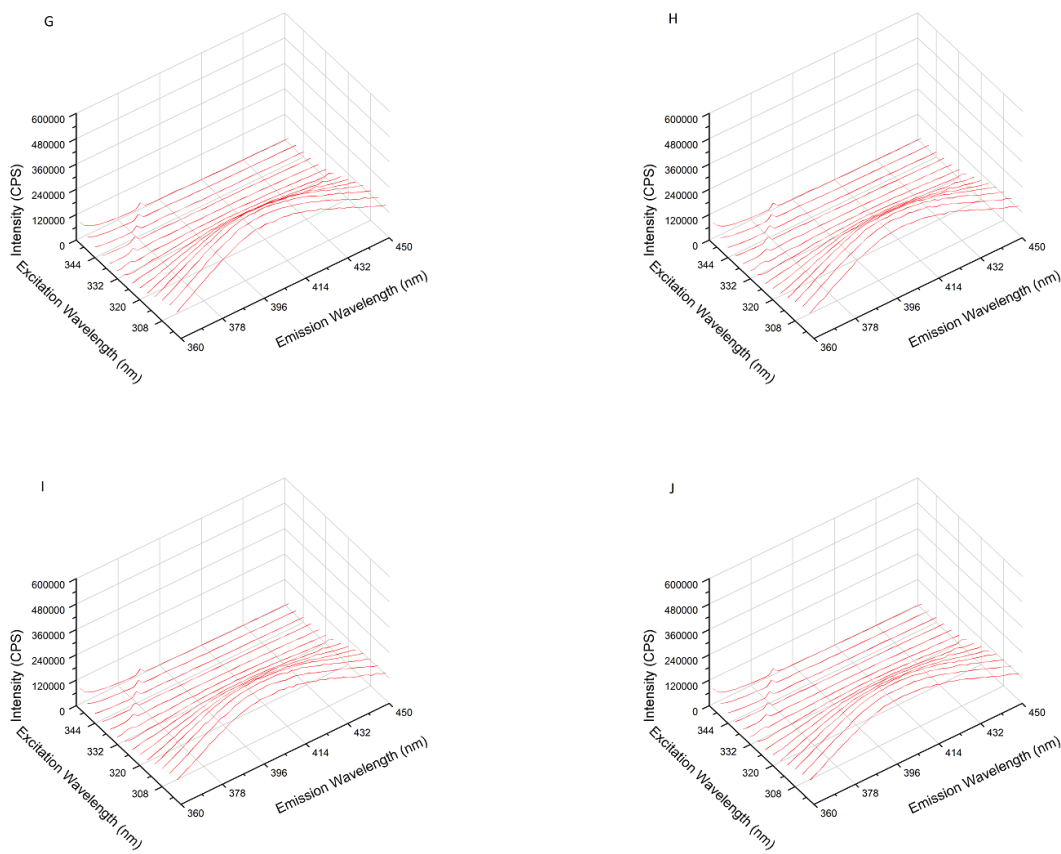
Figure 2.3: 3D luminescence map of (A) pure UiO-66, (B) 0.005, (C) 0.010, (D) 0.015, (E) 0.020, (F) 0.025,(G) 0.030, (H) 0.035, (I) 0.040, (J) 0.045 molar $Ni(NO_3)_2$ solution with UiO-66.

Even though the 3D map provides plenty of information about the luminescence, using it to compare the response from 3 MOFs is very hard. For this end, peak intensities of the 3 MOFs were measures and normalized to ease the comparison between the responses. Each test was repeated enough times and the average was used to represent the peak intensity, and the maximum difference was used as the error. Figure 2.5 shows the peak intensity change of UiO-66, UiO-66-NH_2 and ZrPDA with increasing concentrations of Ni^{2+} ions.
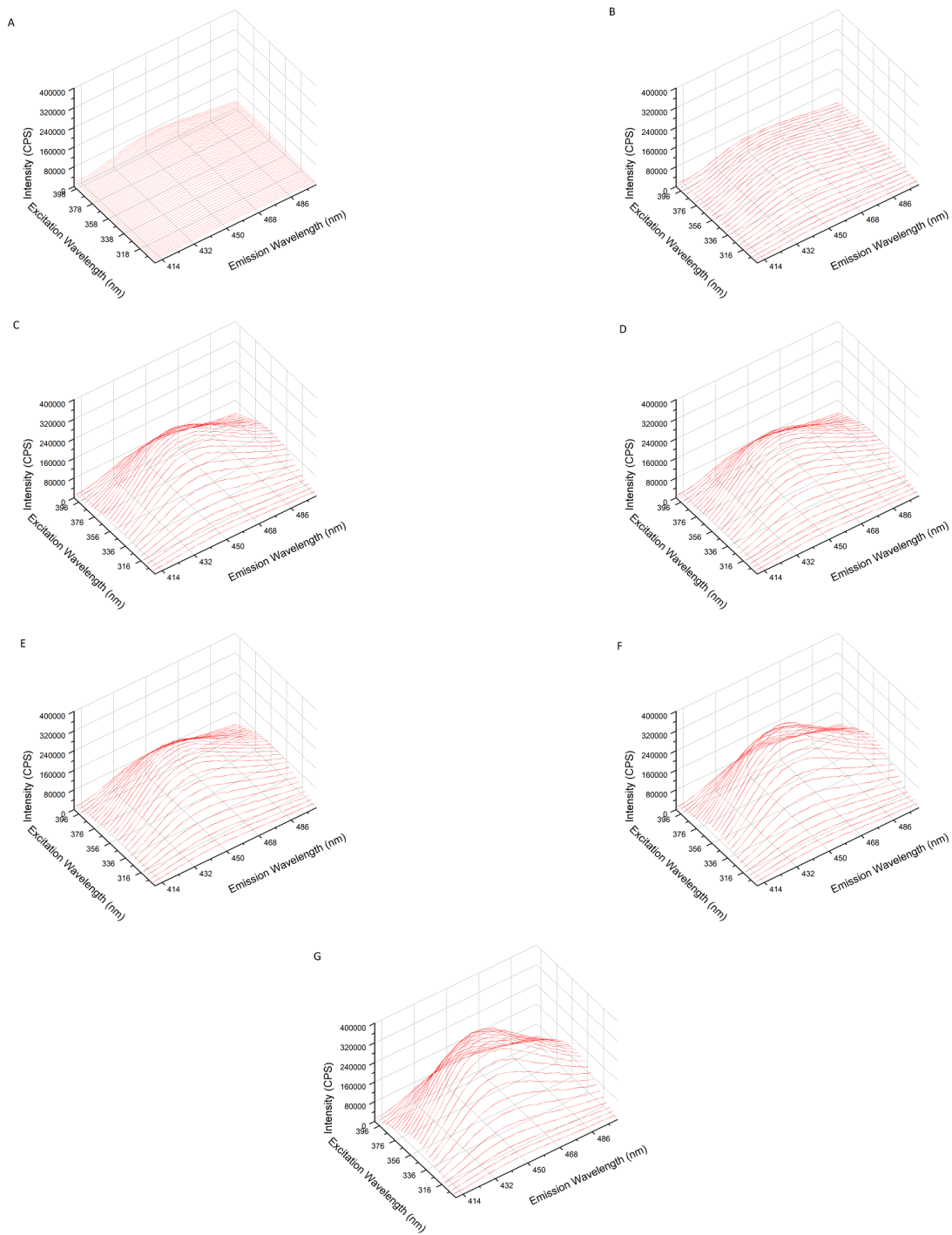
Figure 2.4: 3D luminescence map of UiO-66-NH$_2$ in (A) pure , (B) 0.005, (C) 0.010, (D) 0.015, (E) 0.020, (F) 0.025,(G) 0.030 molar Ni(NO$_3$)$_2$ solution.
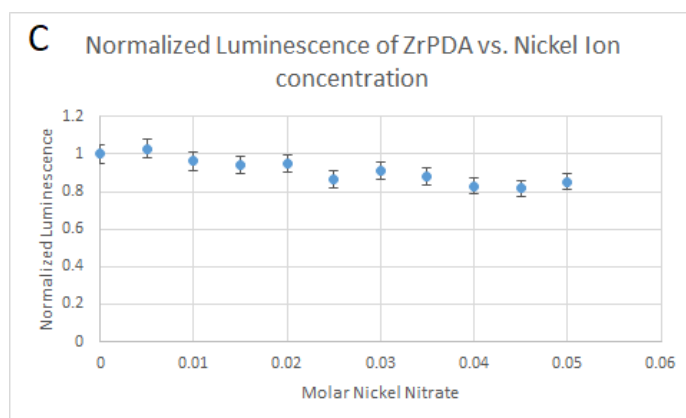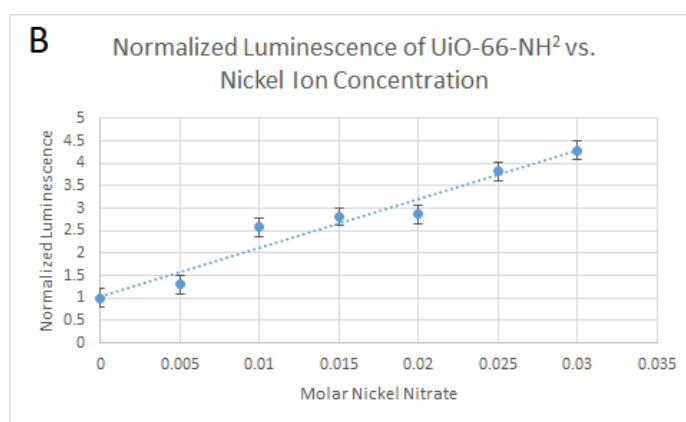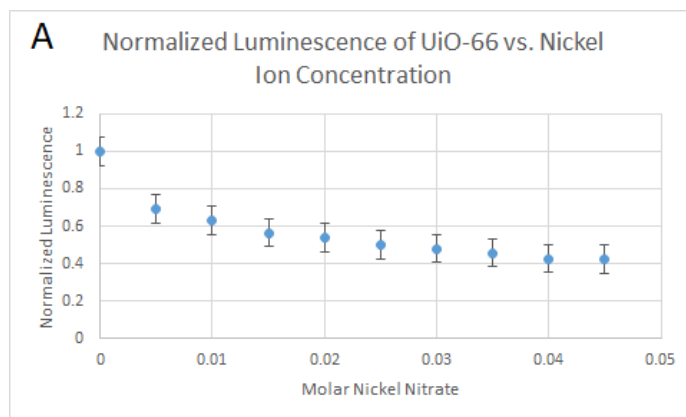
Figure 2.5: Peak luminescence intensity of (A) UiO-66, (B) UiO-66-NH$_2$ and (C) ZrPDA with increasing concentrations of Ni(NO$_3$)$_2$

Copper is the next metal ion that was studied. Copper has similar charge and ionic radius to Ni^{2+}, which makes distinguishing between them much harder and more important. Figures 2.6, 2.7 and 2.8 show the 3D luminescence map of UiO-66, UiO-66-NH_2 and ZrPDA respectively. Similarly to the case of Nickel, comparing the responses from the 3D map is very difficult, as such, Figure 2.9 shows the peak intensity change of (A) UiO-66, (B) UiO-66-NH_2 and (C) ZrPDA. When comparing the responses in Figure 2.9 we can see that all 3 MOFs show a quenching response to addition of Cu^{2+} ions.

UiO-66 shows a very strong quenching response to addition of Copper initially, and the luminescence peak starts to disappear at around 0.2 molar $Cu(NO_3)_2$ and completely disappears at around 0.4 molar $Cu(NO_3)_2$. UiO-66-NH_2 on the other hand shows a relatively linear quenching response, but due to the lower initial peak intensity, the peak disappears at around 0.1 molar $Cu(NO_3)_2$. ZrPDA shows a strong quenching response initially, but quenching gets smaller at higher concentrations, and the peak does not disappear at concentrations as high as 0.35 molar $Cu(NO_3)_2$.

The enhancing effect of Ni^{2+} on UiO-66-NH_2 is very different from the quenching effect of Cu^{2+}, and we propose that this difference can be used to increase the factor of confidence when reporting concentration of Ni^{2+} ions.

It is also important to note that even though metal ions were dissolved in DI water, trace amounts of ions in addition to the effects of water and other environmental effects cause a background noise. Because of this noise, very low intensities such as the case for UiO-66 in a 0.4 molar $Cu(NO_3)_2$ solution (Figure 2.6.N) are less reliable. Since the amount of intensity due to water is relatively constant, it is advised to take steps to ensure luminescence doesn't fall below a certain threshold.
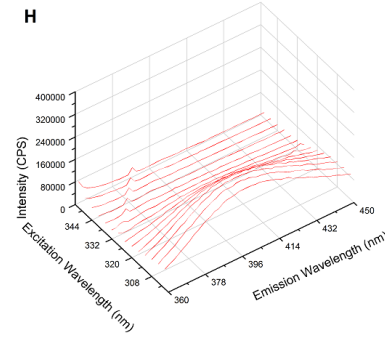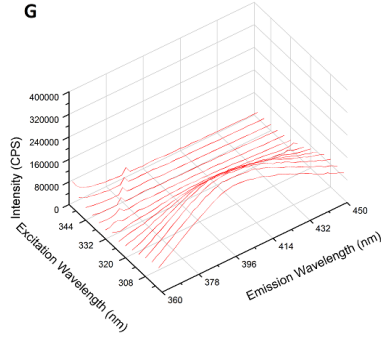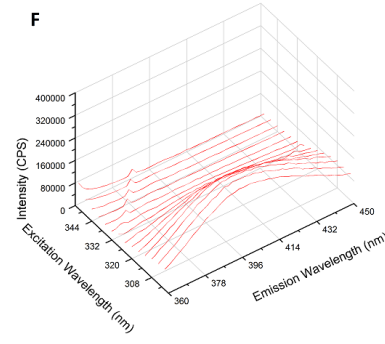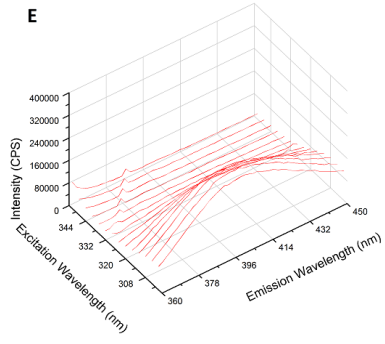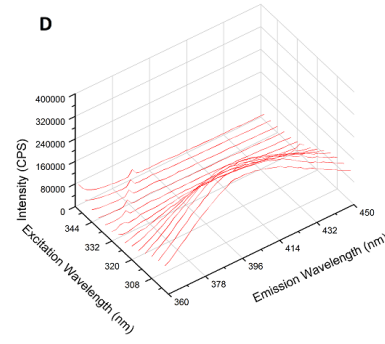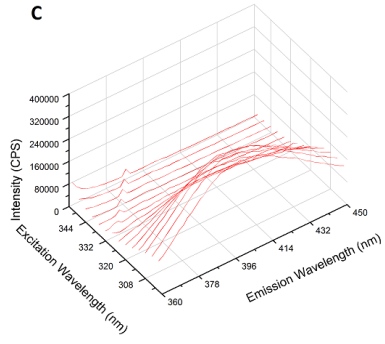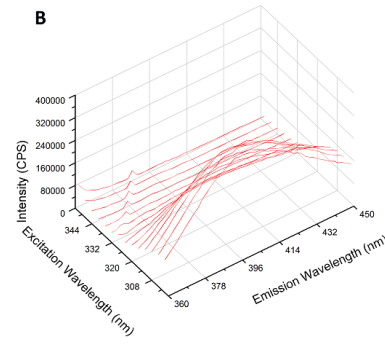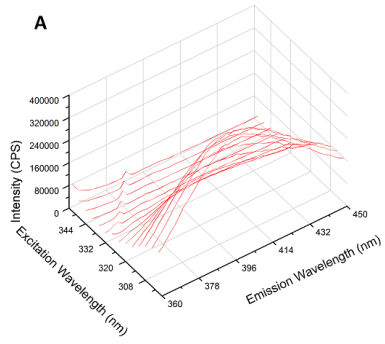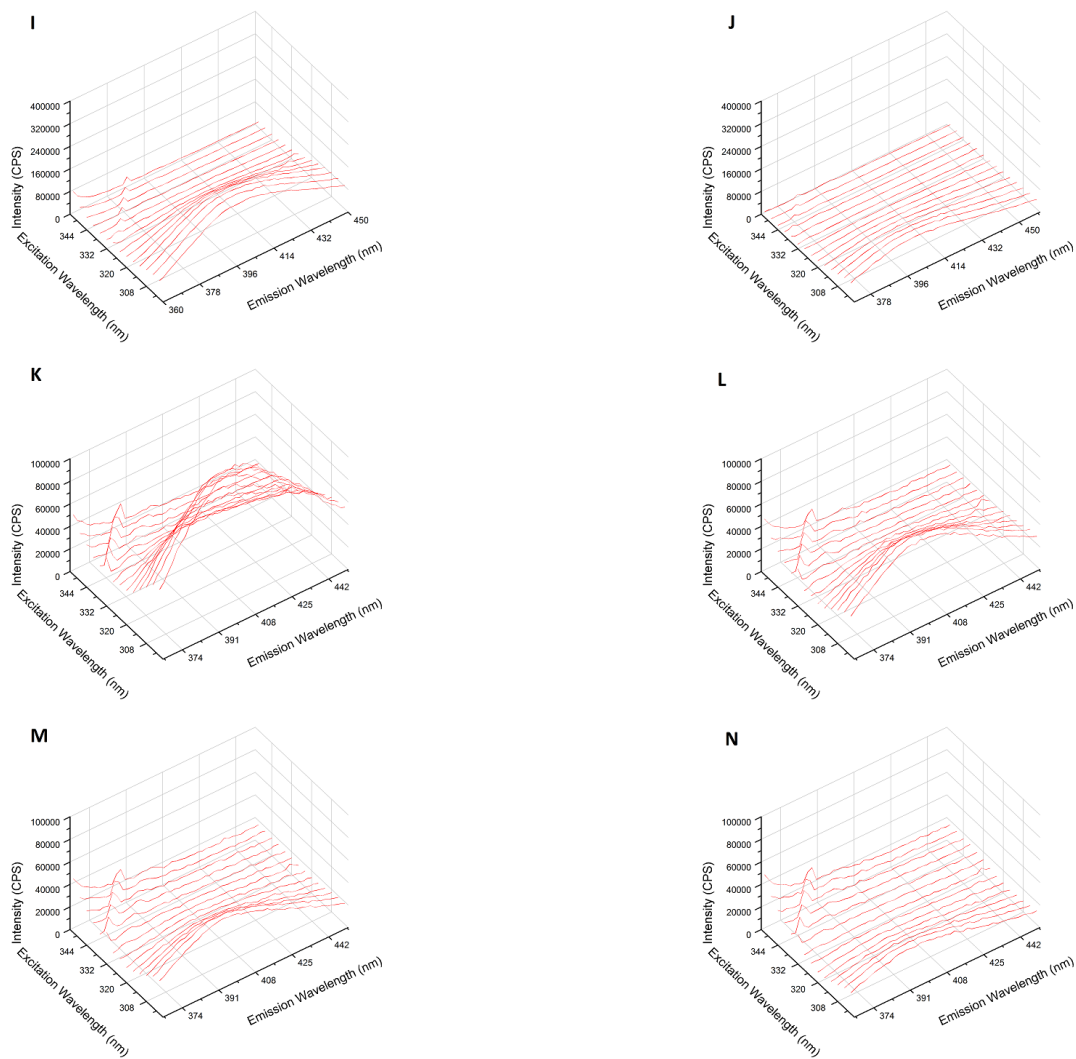
Figure 2.6: 3D luminescence map of (A) 0.005, (B) 0.010, (C) 0.015, (D) 0.020, (E) 0.025,(F) 0.030, (G) 0.035, (H) 0.040, (I) 0.045, (J) 0.050 molar $Cu(NO_3)_2$ solution with UiO-66, with Y-axis set at 400000 intensity. (K) 0.10, (L) 0.20, (M) 0.30 and (N) 0.40 Molar molar $Cu(NO_3)_2$ solution with UiO-66, with Y-axis set at 100000 intensity.
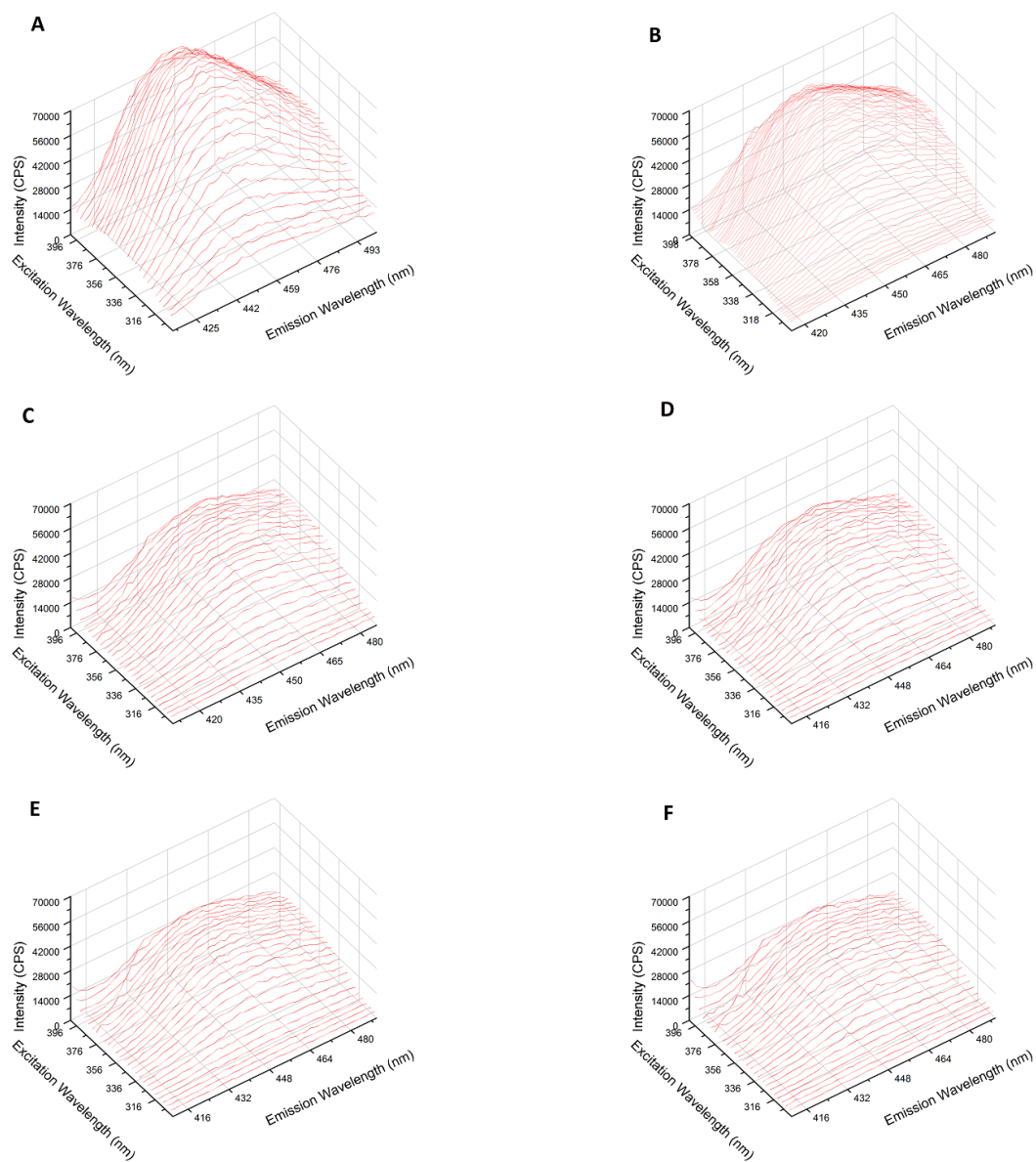
Figure 2.7: 3D Luminescence map of UiO-66-NH$_2$ in (A) Pure, (B) 0.005, (C) 0.010, (D) 0.015, (E) 0.020, (F) 0.025 molar Cu(NO$_3$)$_2$ solution
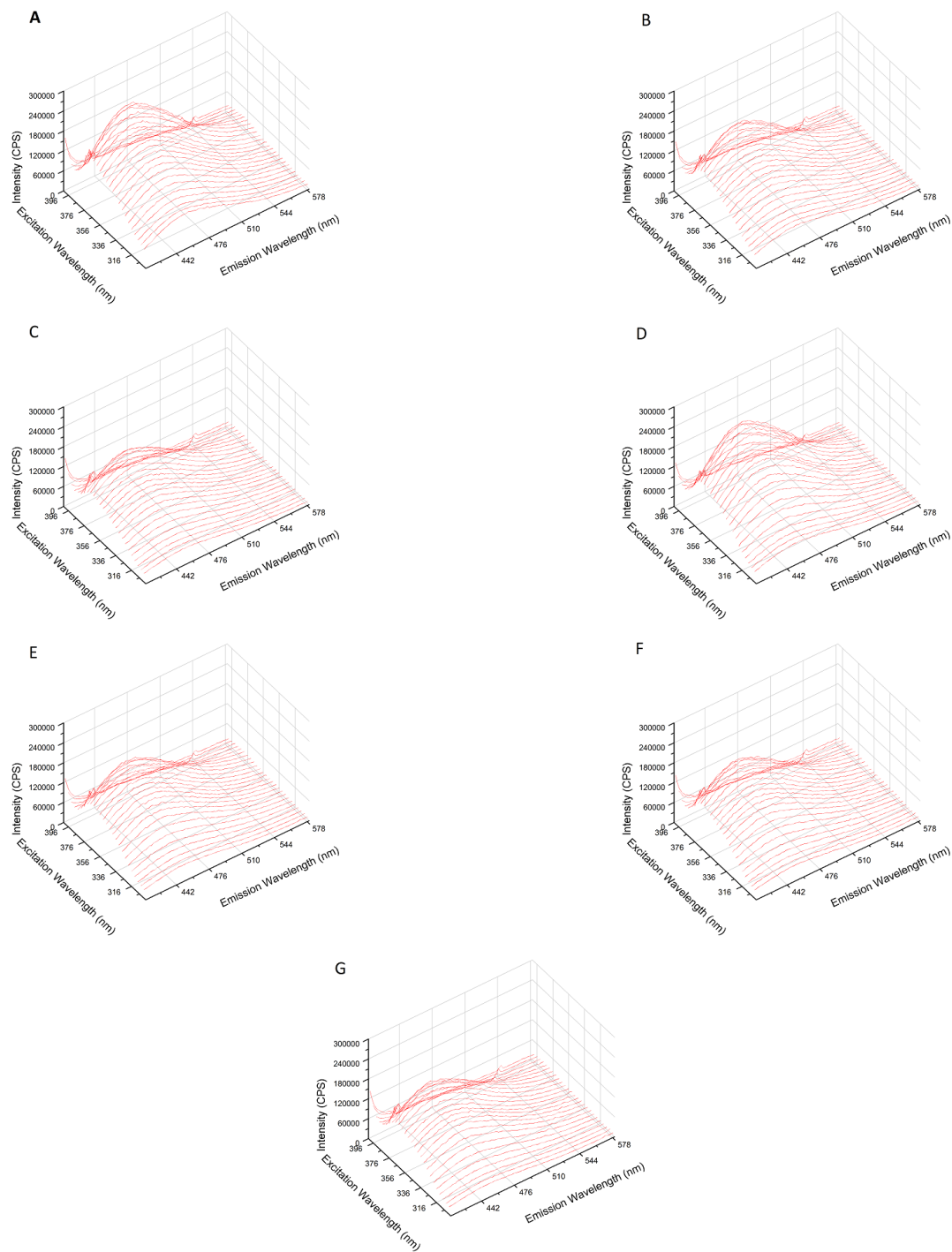
Figure 2.8: 3D Luminescence map of ZrPDA in (A) 0.05, (B) 0.10, (C) 0.15, (D) 0.20, (E) 0.25, (F) 0.30 and (G) 0.35 molar $Cu(NO_3)_2$ solution

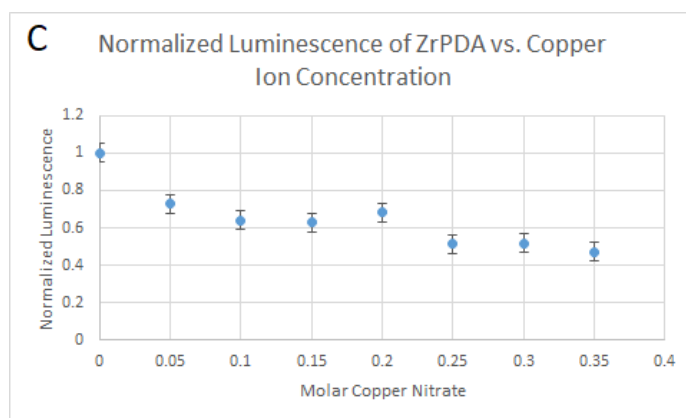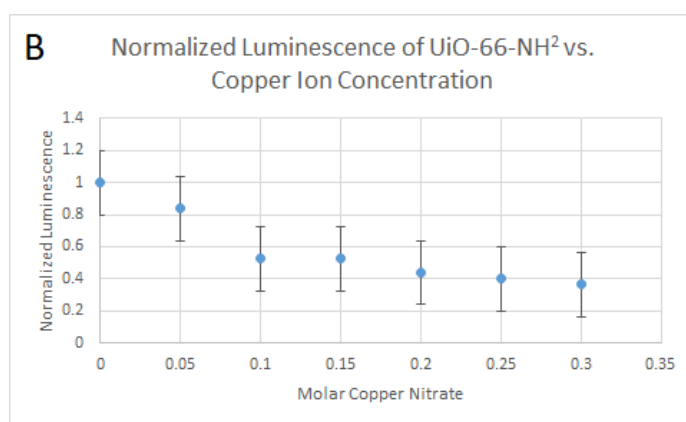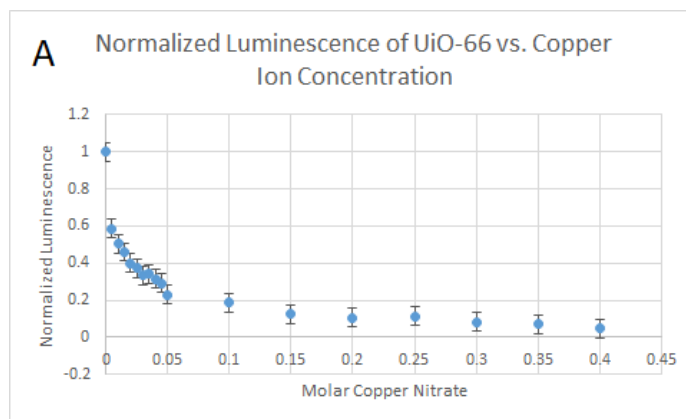Figure 2.9: Peak luminescence intensity of (A) UiO-66, (B) UiO-66-NH$_2$ and (C) ZrPDA with increasing concentrations of Cu(NO$_3$)$_2$

The combination of the very dangerous effects of Lead poisoning reported by Needleman (2004), in addition to the fact reported by Sampson and Winter (2016) that Lead poisoning disppropotionately affects minorities and people in poverty, makes Lead detection crucial. One of the obsticles in the way of detecting Lead using Luminescence MOFs is the difficulty to distinguish between Lead and other ions.

Normalized luminescence of UiO-66, UiO-66-NH_2 and ZrPDA when in contact with increasing concentrations of $Pb(NO_3)_2$ is shown in Figures 2.10, 2.11 and 2.12 respectively. Luminescence of ZrPDA does not seem be affected by introduction of Lead to the system, while UiO-66 shows the expected quenching response. On the other hand, UiO-66-NH_2 shows a very unique response. At first, the expected enhancing effect is observed. But the enhancing region is followed by a quenching region and finally a saturated luminescence that does not change that much with increasing the concentration of Lead. To ensure that an error was not causing this peculiar behaviour, the tests were repeated several times, but the results were consistent. To the best of the author's knowledge, no other group has tested UiO-66-NH_2 in contact with such high concentrations of Lead. More research on the cause of this strange behaviour is needed before a solid conclusion about the reason behind it can be made. Although the safe levels of Lead in water are far below the conc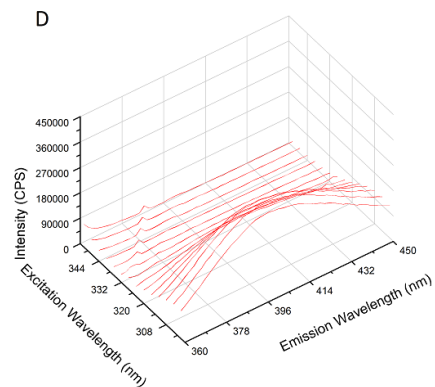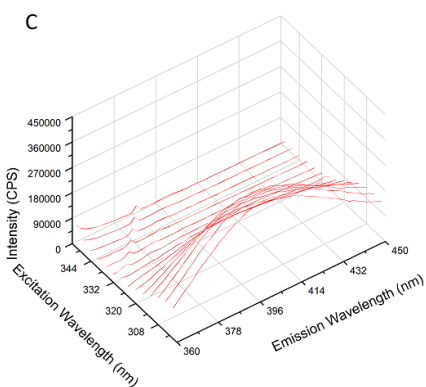entrations that cause this response, it is important to study this phenomenon to ensure similar situations do not occur, or to be prepared for the possible error to the readings.

Figure 2.13 compares the peak intensity of UiO-66, UiO-66-NH_2 and ZrPDA. Concentration of Lead was not increased passed 0.05 Molar for UiO-66 and ZrPDA since no visible change was observed.
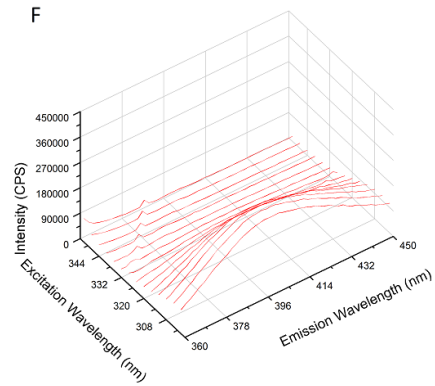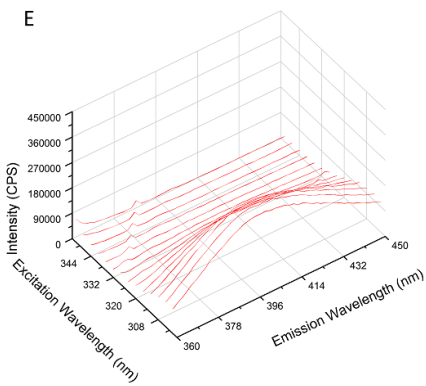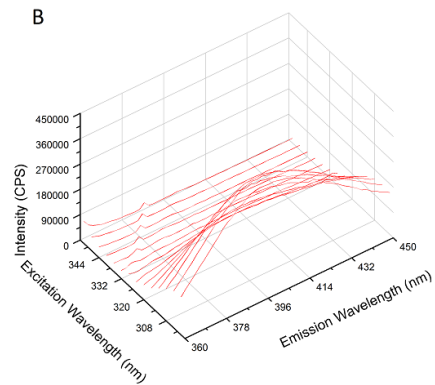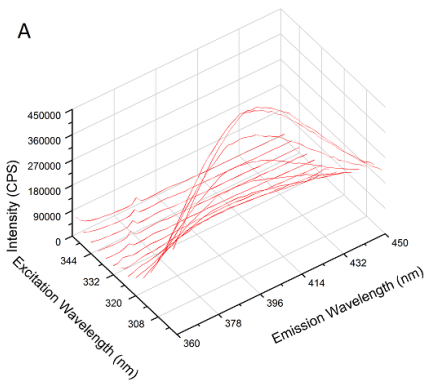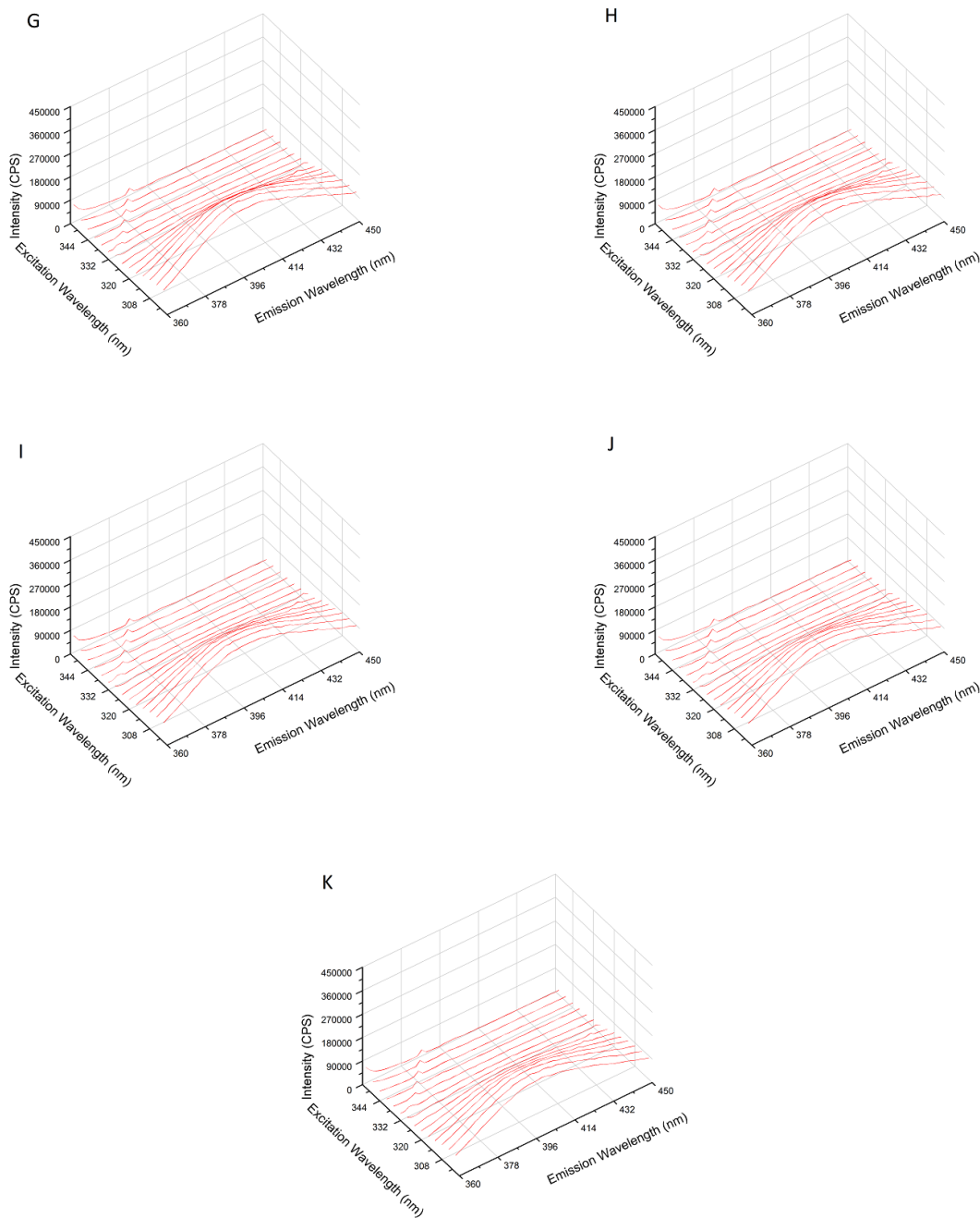
Figure 2.10: 3D luminescence map of UiO-66 in a solution containing (A) Pure, (B) 0.005, (C) 0.010, (D) 0.015, (E) 0.020,(F) 0.025, (G) 0.030, (H) 0.0350, (I) 0.040, (J) 0.045 and (K) 0.050 molar $Pb(NO_3)_2$
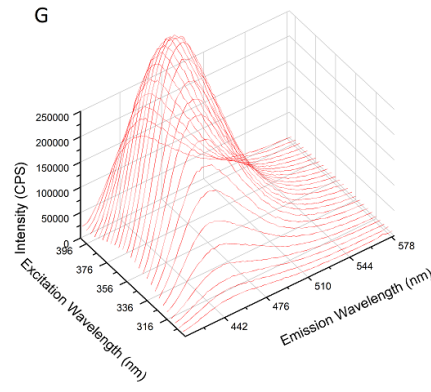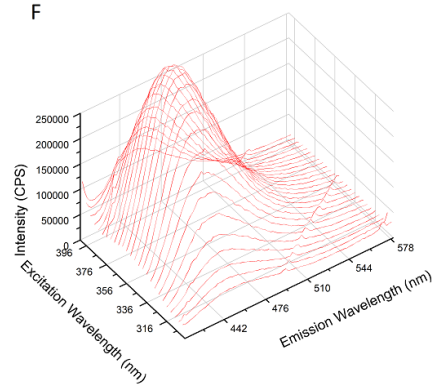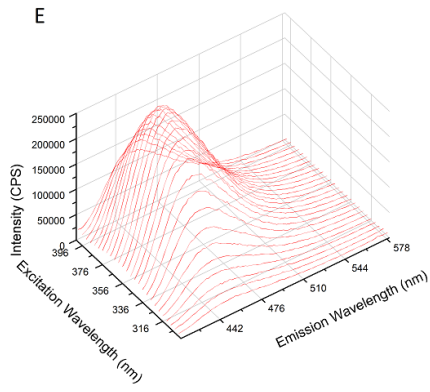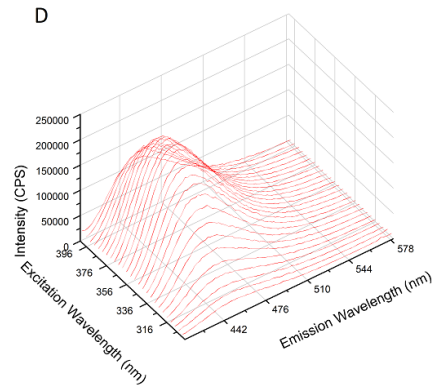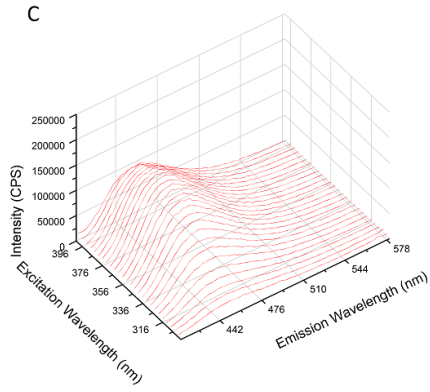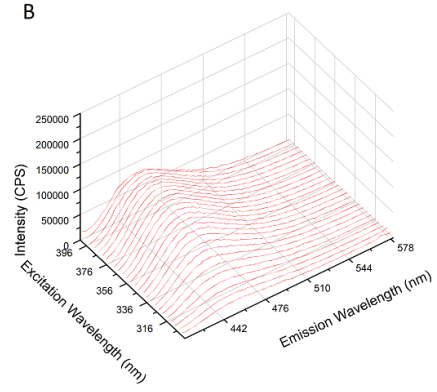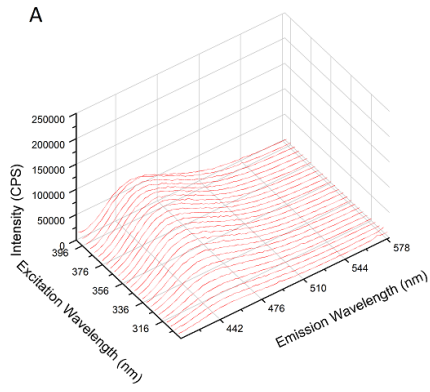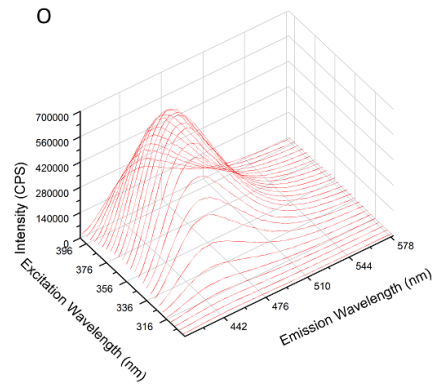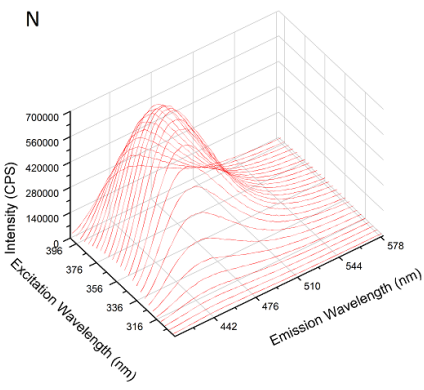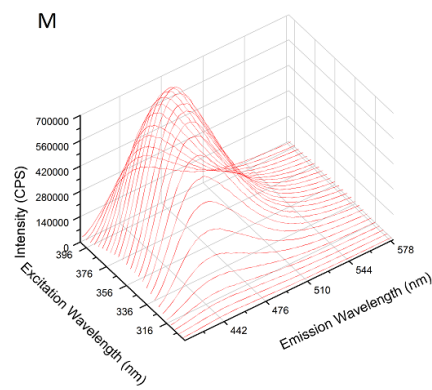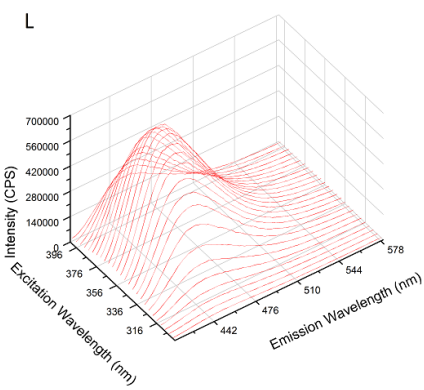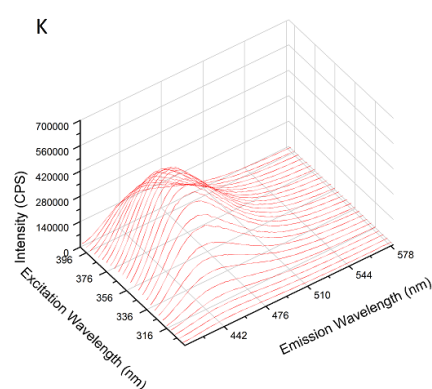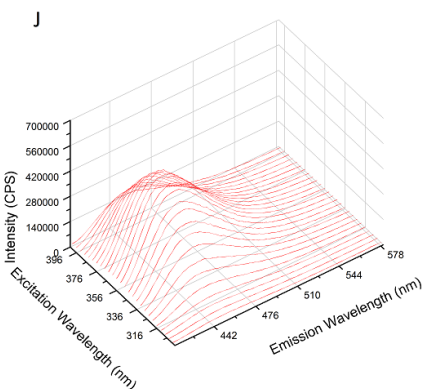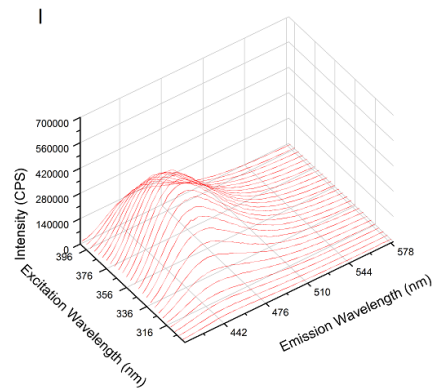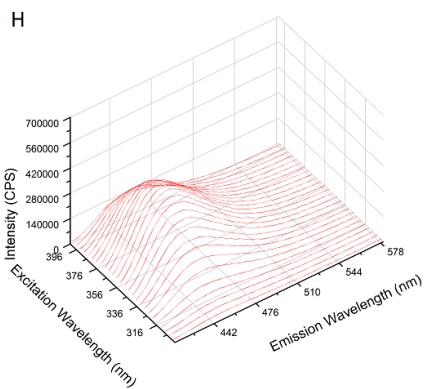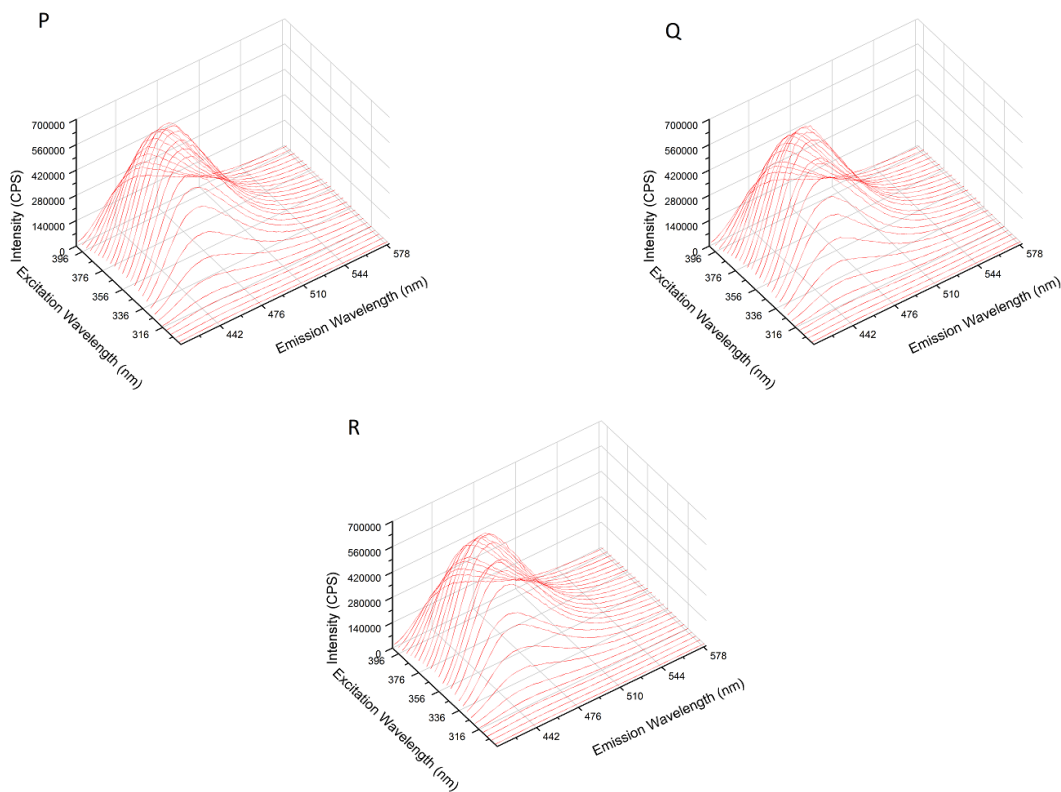
Figure 2.11: 3D Luminescence map of UiO-66-NH$_2$ in (A) Pure, (B) 0.005, (C) 0.010, (D) 0.015, (E) 0.020, (F) 0.025, (G) 0.030, (H) 0.035, (I) 0.040, (J) 0.045, (K) 0.050, (L) 0.100, (M) 0.150, (N) 0.200, (O) 0.250, (P) 0.300, (Q) 0.350 and (R) 0.400 molar Pb(NO$_3$)$_2$ solution. The intensity axis is set at 250,000 from A to G, and at 700,000 from H to R to better show regional changes in luminescence
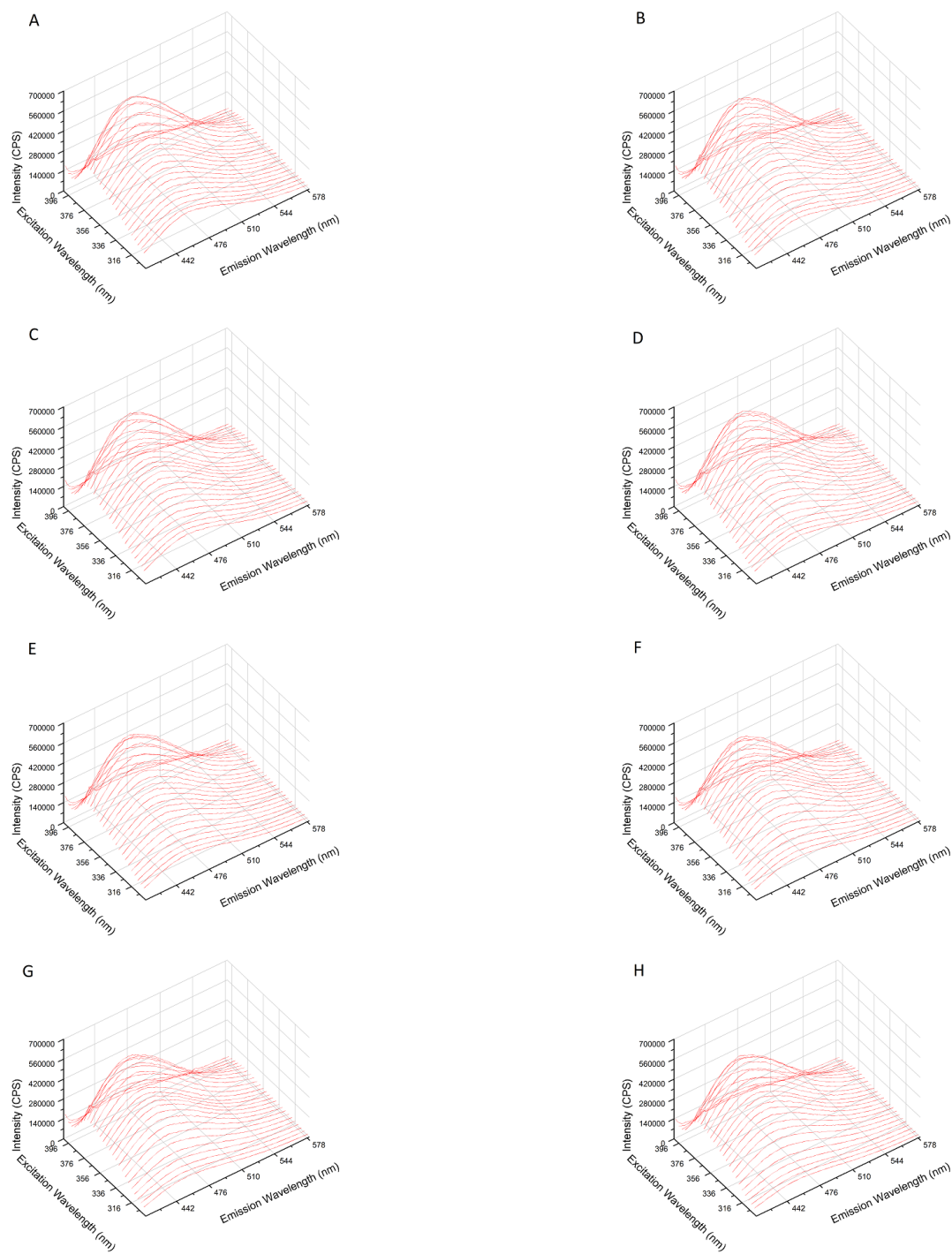
Figure 2.12: 3D Luminescence map of ZrPDA in (A) pure, (B) 0.005, (C) 0.010, (D) 0.030, (E) 0.050, (F) 0.100, (G) 0.150 and (H) 0.200 molar $Pb(NO_3)_2$ solution
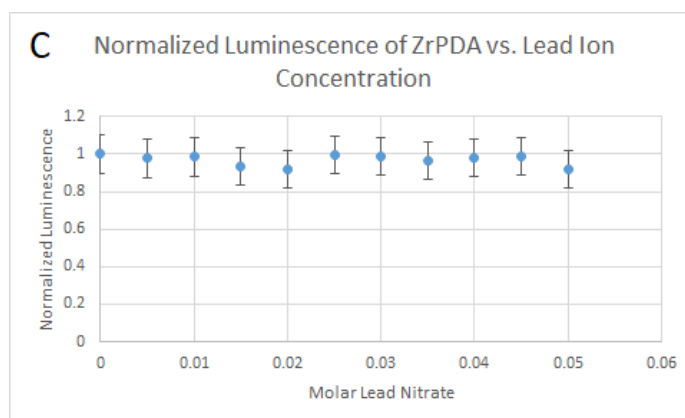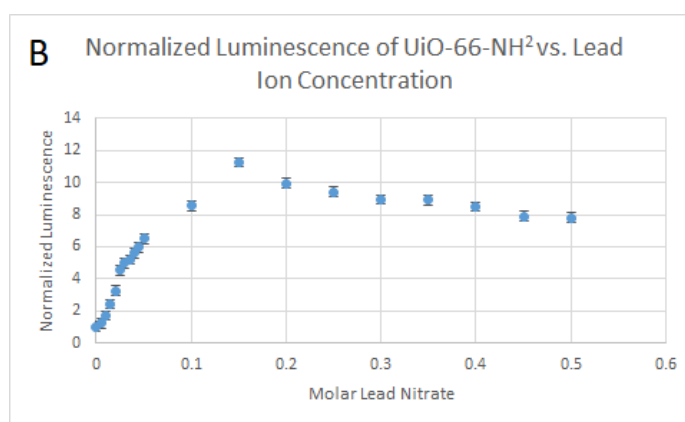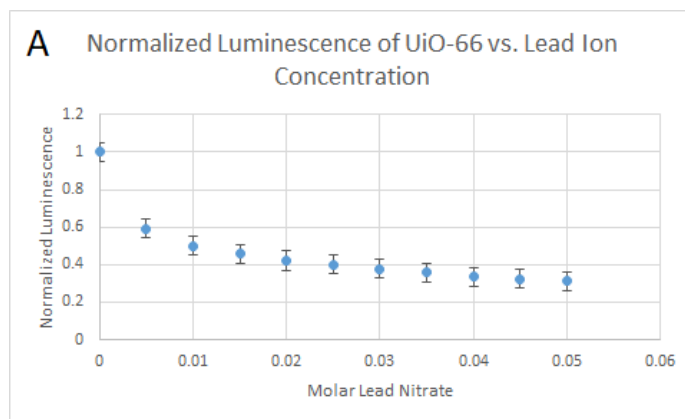
Figure 2.13: Peak luminescence intensity of (A) UiO-66, (B) UiO-66-NH$_2$ and (C) ZrPDA with increasing concentrations of Pb(NO$_3$)$_2$

The last ion that was studied is Barium. Barium has the same charge and period on the periodic table as Lead, and for most of luminescent MOF detectors, it is very difficult to tell it apart from other ions. Even though Barium is not very prevalent in most drinkable water sources, the similarities it has with the other 3 ions could provide us with better understanding of the luminescence responses.

As can be seen in figure 2.14, UiO-66 luminescence response shows a very strong initial quenching until 0.05 Molar Barium concentration, followed by a saturated region in which luminescence does not change with increasing concentration. Luminescence intensity in UiO-66-NH_2 as shown in Figure 2.15 shows a relatively linear increase until 0.2 molar $Ba(NO_3)_2$, above which the luminescence is too strong for the detector that was used, and the tests were not continued. Barium does not show the same affect on luminescence as Lead, and luminescence is not quenched after 0.15. Adding Barium to ZrPDA shows a similar result to adding Lead, and even though a small amount of quenching can be seen here, the amount is so low that it is not usable. Figure 2.16 shows 3D luminescence map of ZrPDA with increasing concentrations of $Ba(NO_3)_2$. Figure 2.17 compares the luminescence peak intensity of UiO-66, UiO-66-NH_2 and ZrPDA with increasing concentrations of Barium.

Comparing Figures 2.17, 2.13, 2.9 and 2.5, gives us a very good understanding of how introduction of each ion will affect the luminescence of the 3 MOFs used in this research.

A   B

C   D

E   F

G   H

35
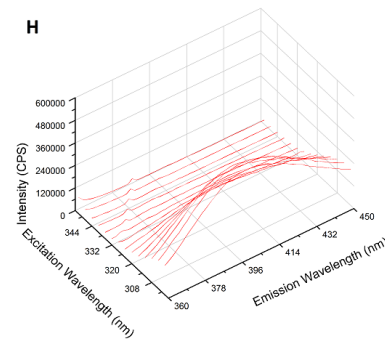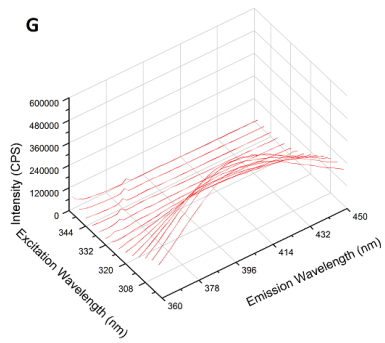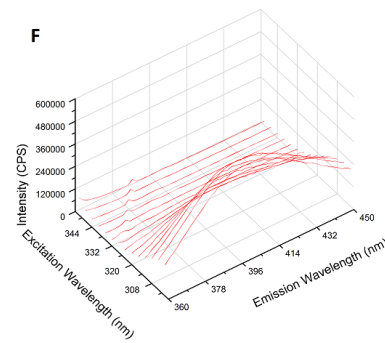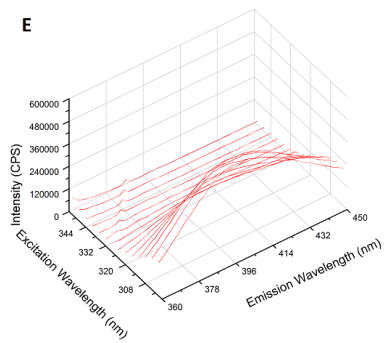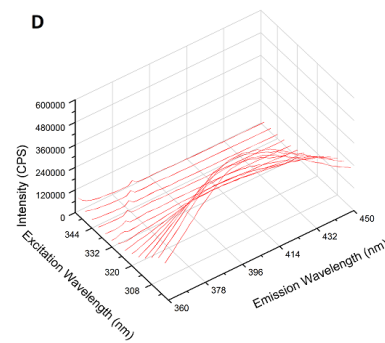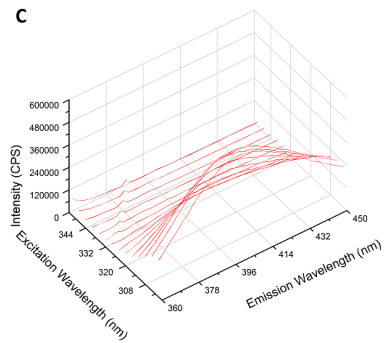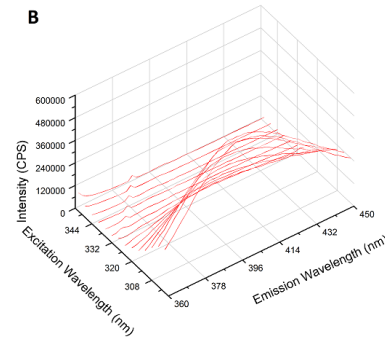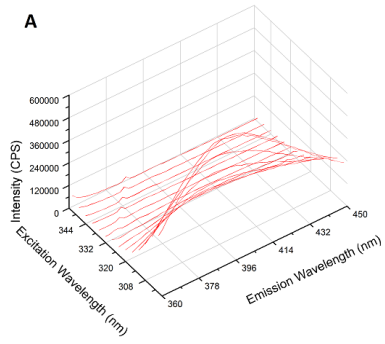
Figure 2.14: 3D luminescence map of UiO-66 in a solution containing (A) DI water, (B) 0.005, (C) 0.010, (D) 0.015, (E) 0.020, (F) 0.025, (G) 0.030, (H) 0.035, (I) 0.040, (J) 0.045, (K) 0.050, (L) 0.150 and (M) 0.250 molar $Ba(NO_3)_2$
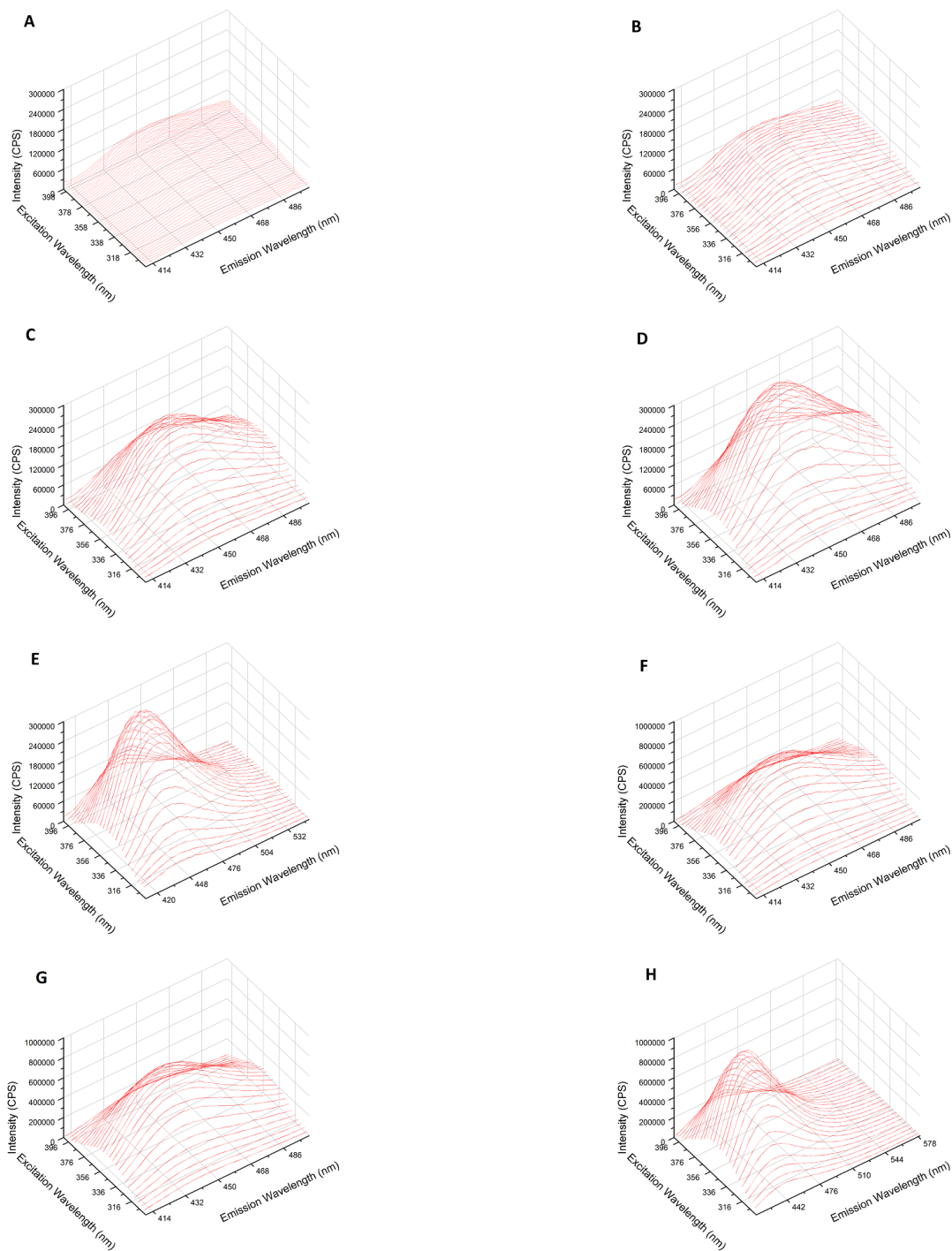
Figure 2.15: 3D luminescence map of UiO-66-NH$_2$ in a solution containing (A) DI water, (B) 0.010, (C) 0.020, (D) 0.030, (E) 0.050, (F) 0.100, (G) 0.150 and (H) 0.200 molar Ba(NO$_3$)$_2$. Figures (F), (G) and (H) have a different Y-axis set at 1,000,000.
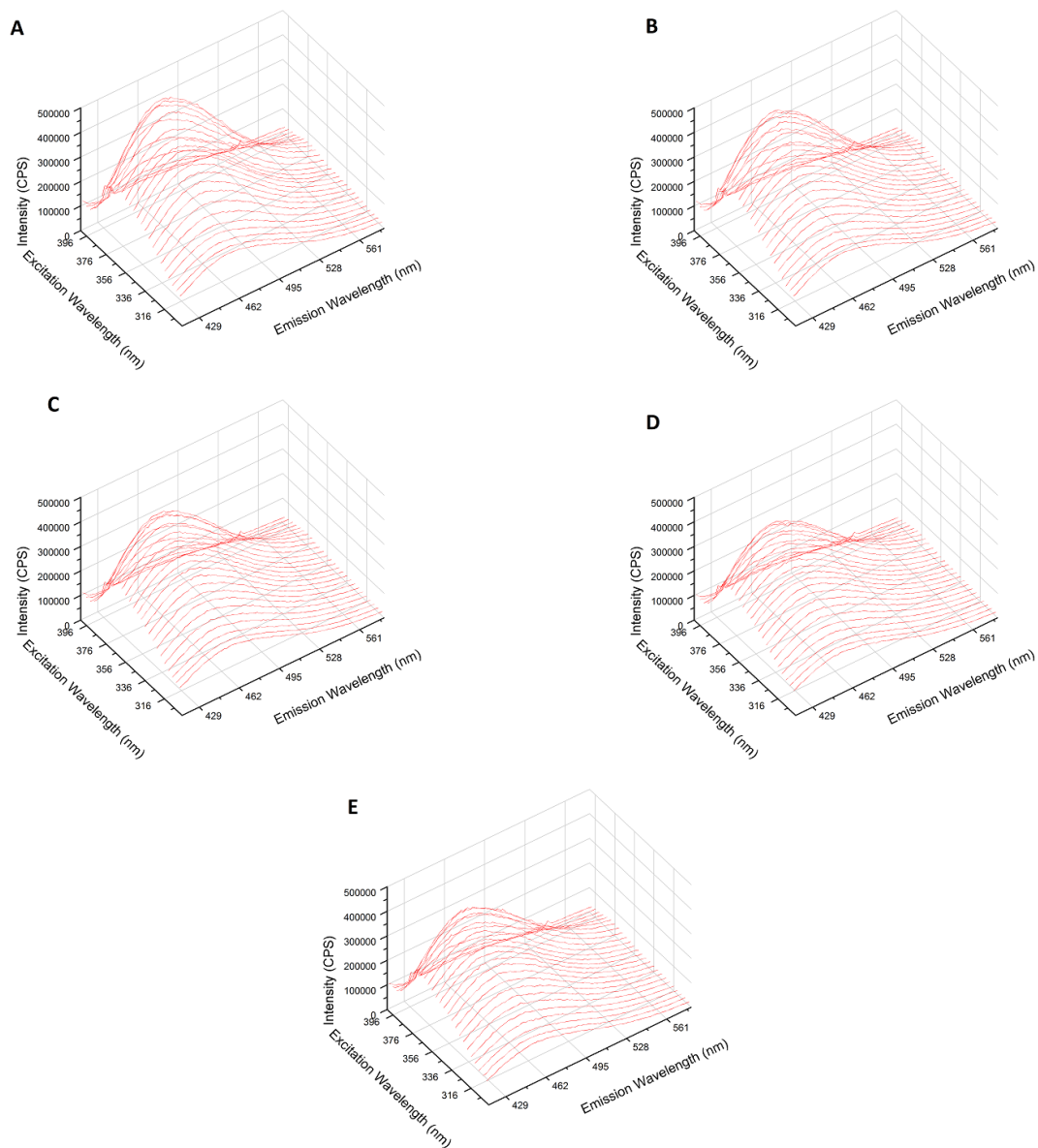
Figure 2.16: 3D luminescence map of ZrPDA in a solution containing (A) DI water, (B) 0.05, (C) 0.10, (D) 0.15 and (E) 0.20 molar $Ba(NO_3)_2$
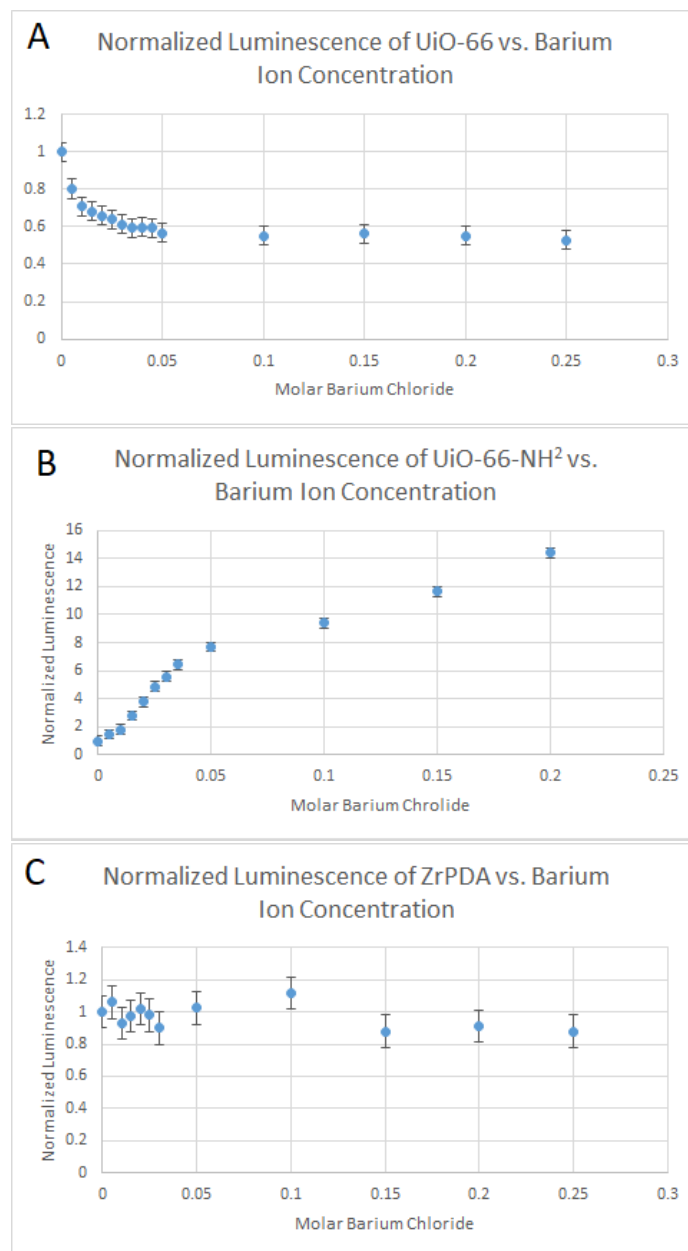
Figure 2.17: Luminescence peak intensity of (A) UiO-66, (B) UiO-66-NH$_2$ and ZrPDA with increasing concentrations of Barium

After studying the response from introduction of a single metal ion to a solution containing a single MOF, it is possible to compare the results to a system containing two MOFs.

While in theory it is possible to combine any two MOFs and study the results, it is not advised to randomly combine any ratio of them together. As such, the first step was to find the perfect combination for a MOF pair. The combination requires to have the peak from both MOFs present, so that the change in peak intensity and position can be studied. ZrPDA and UiO-66 both have similar intensity for their peak in DI water, so the first mixture that was studied was ZrPDA+UiO-66.

Even though the intensity of their peaks is relatively the same, introduction of the new MOF has a very strong effect on the intensity of the first peak. Figure 2.18 shows 3D luminescence map of the mixture with increasing concentrations of ZrPDA. Unlike what might be expected, the best combination is not the 1:1 ratio of these MOFs, rather 20:12 ratio of UiO-66 to ZrPDA. As the amount of ZrPDA is increased, the peak for UiO-66 (located at 300,394 nm) starts to quench, and the peak for ZrPDA (located at 372,450 nm) is getting stronger. Since UiO-66 also has a strong luminescence around 372,450, and also since UiO-66 and ZrPDA are affecting each other's luminescence, a peak shift can be observed to (300,400 nm) for UiO-66 and (368,458) for ZrPDA. increasing the ratio to 20:20 will quench the peak for UiO-66 even more, and enhance the peak for ZrPDA.
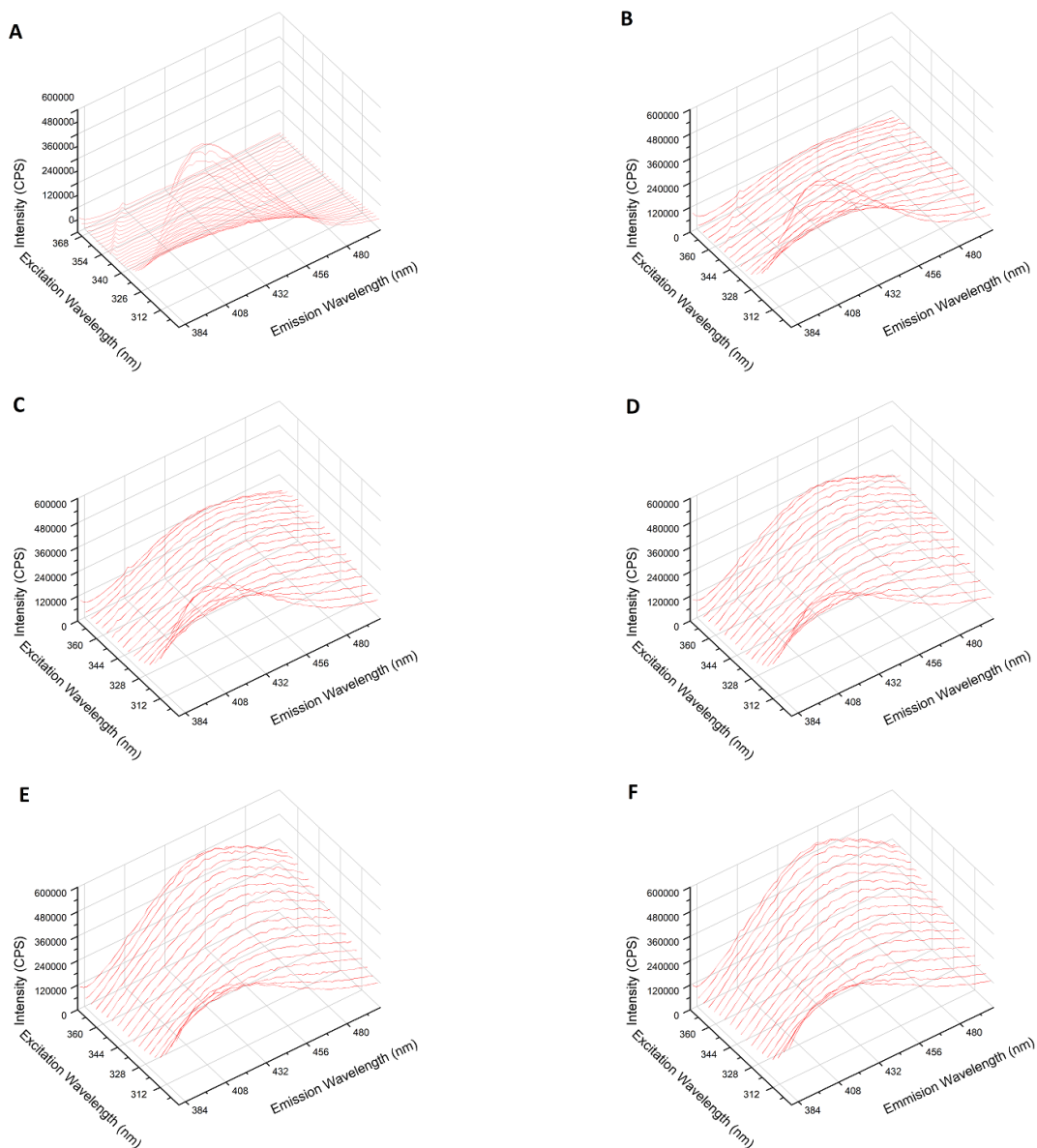
Figure 2.18: 3D luminescence map of 20 mg UiO-66 and (A) 0, (B) 4, (C) 8, (D) 12, (E) 16 and (F) 20 mg ZrPDA

Barium was the first metal ion to be tested. It was expected for the peak for UiO-66 to be quenched initially and the peak for ZrPDA to not change that much. The results however, were very different. The peak for UiO-66 shows a small amount of enhancing and a peak shift for emission from ~ 400 nm to around 410. The peak

for ZrPDA shows a small amount of enhancing as well, but the height of the peak gets smaller, until 0.015 molar $Ba(NO_3)_2$, after which the peak is removed as the rest of the map is getting enhanced. However, the strangest change comes at around excitation of 320 and emission of 416. This peak that didn't exist for the mixture in DI water, starts to appear around 0.010 molar $Ba(NO_3)_2$, and even overtakes the other peaks at 0.020 molar $Ba(NO_3)_2$, and is too strong above that for our detector. It seems that this very strong and Barium sensitive luminescence peak, exists in systems containing metal ions and a mixture of ZrPDA and UiO-66. Since the reason for this peak, or the mechanism of luminescence is not determined, it is not possible to determine the reason for the enhancement of any of the 3 peaks. But, the huge change in luminescence response in concentrations as low as 0.005 molar can be very useful to detect low concentrations of Barium ions. Figure 2.19 shows the 3D luminescence map of UiO-66+ZrPDA in a solution with increasing concentrations of $Ba(NO_3)_2$.

Figure 2.19: 3D luminescence map of 20 mg UiO-66 and 12 mg ZrPDA in a solution containing (A) DI water, (B) 0.005, (C) 0.010, (D) 0.015, (E) 0.020 and (F) 0.025 molar $Ba(NO_3)_2$

In case of Copper, there are 4 points of interest on the luminescence map. First, is the (300,$\sim$ 400 nm) point on the luminescence map. This point corresponds to the peak for UiO-66. This point, similar to what occurs in Figure 2.9.A, shows a quench-

ing response to addition of $Cu(NO_3)_2$. Second point of interest is the (368,458 nm) point corresponding to the peak for ZrPDA. This point also shows a small quenching similar to the case of Figure 2.9.C, but it is saturated after 0.01 molar $Cu(NO_3)_2$. The other two points of interest are (320,410 nm) and (344, 410 nm). These two peaks that did not exist in Figure 2.20.A, show an initial enhancing until 0.010 molar $Cu(NO_3)_2$, but after that they are quenched until being saturated. It is possible that the reason for this phenomenon is that these two peaks require metal ions in water to be activated. So, initially increasing the concentration of Copper ions activates the mechanism for the luminescence at these positions. But after that, the expected quenching effect of Copper is observed. This is just a hypothesis and further investigation of this response is required.
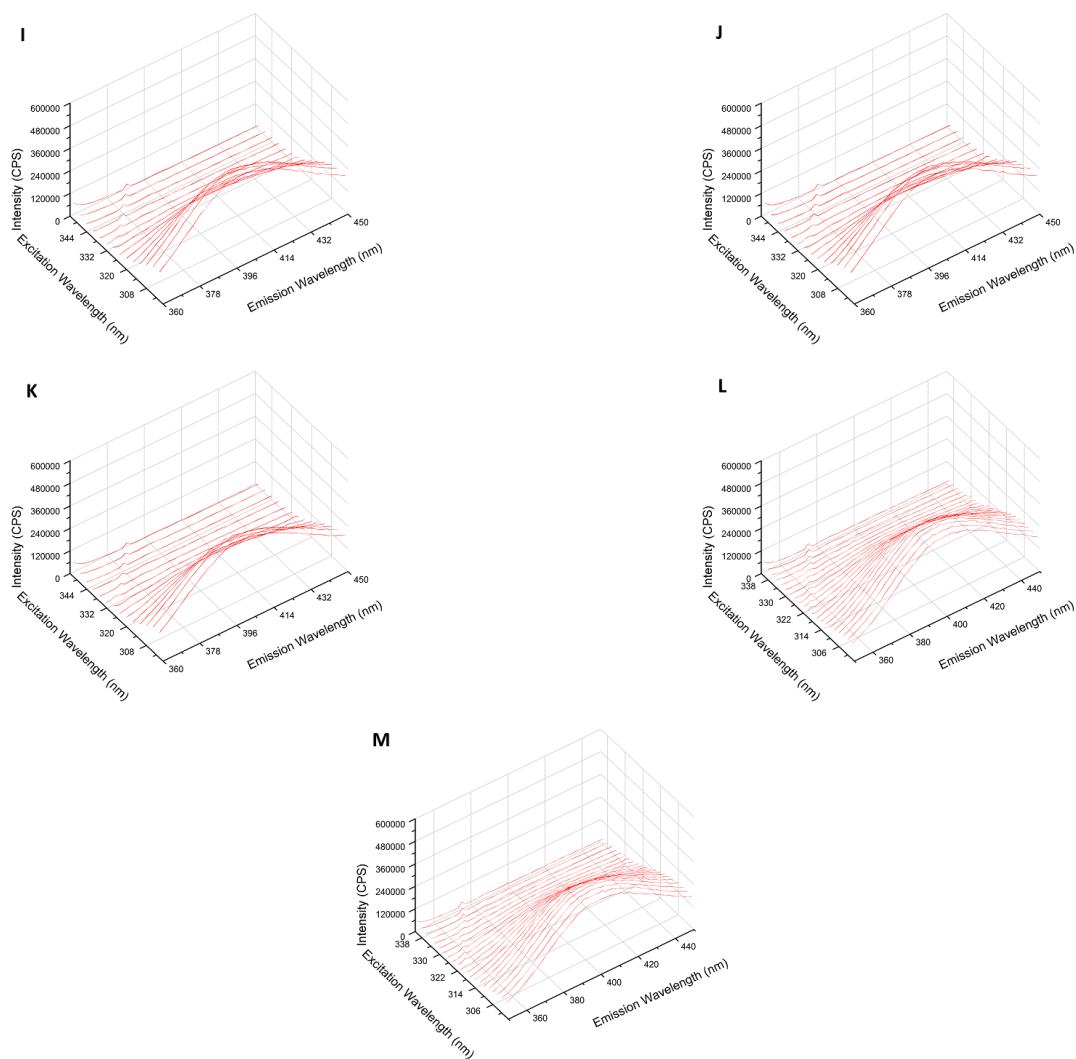
Figure 2.20: 3D luminescence map of 20 mg UiO-66 and 12 mg ZrPDA in a solution containing (A) DI water, (B) 0.005, (C) 0.010, (D) 0.015, (E) 0.020, (F) 0.025, (G) 0.030, (H) 0.035 and (I) 0.040 molar $Cu(NO_3)_2$

In case of Lead and Nickel, there are 3 points of interest. The peak corresponding to UiO-66, the peak corresponding to ZrPDA and the peak located at ($\sim$ 320,410 nm) which is activated after metal ions are introduced. In the UiO-66+ZrPDA+Ni

system, the peak for UiO-66(located at 300,410 nm) shows very little quenching which is too small and is negligible. The point of interest corresponding to ZrPDA (located at 368,458 nm) shows little to no change with increasing concentrations of Nickel, similar to the case observed in Figure 2.5.C. The third point of interest, located at (320,414 nm) shows very strong enhancing effect initially until 0.01 molar $Ni(NO_3)_2$, after which the intensity remains constant. It can be hypothesized that the (320,414 nm) is metal activated, but Nickel ions have no quenching or enhancing effect on it. Figure 2.21 shows the 3D luminescence map of the MOF mixture with increasing concentrations of Nickel.

In case of Lead, the point of interest corresponding to UiO-66 shows no consistent change with increasing concentrations of Lead ions. The point of interest corresponding to ZrPDA shows a small amount of initial enhancing, but it remains the same afterwards. After introducing Lead metal ions, it's neighboring points have a higher intensity, which means there is no longer a peak at that position. However, the third point of interest shows a strong initial enhancing, followed by a quenching and a saturation region. It can be hypothesized that in this case, similar to some of the ones before, the first enhancing region is due to activation of the luminescence mechanism at (320,410 nm), but after 0.01 molar $Pb(NO_3)_2$, Lead ions have a quenching effect until the system is saturated, and increasing the amount of Lead has no effect on luminescence. Figure 2.22 shows the 3D luminescence map of the MOF mixture with increasing concentrations of Lead.
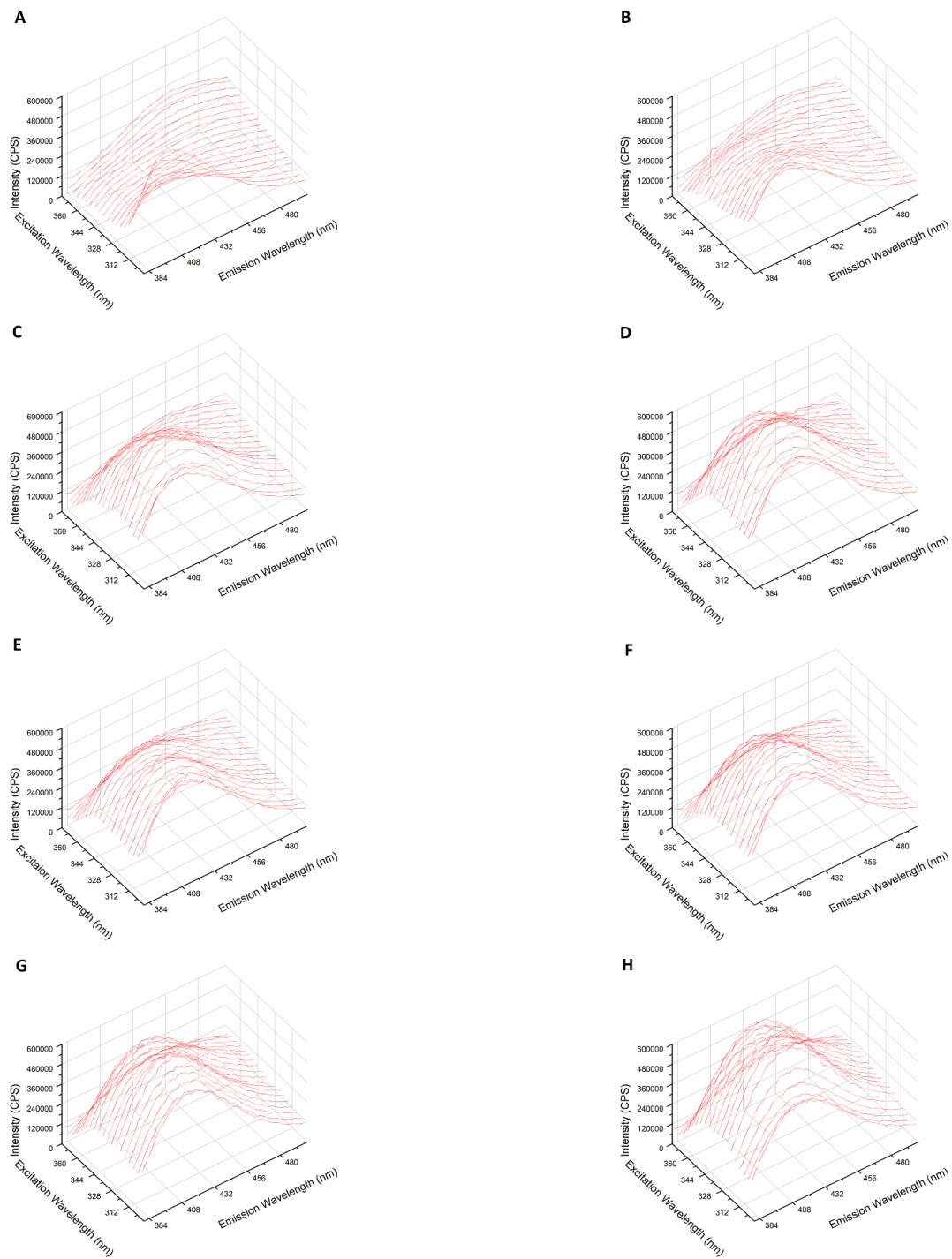
Figure 2.21: 3D luminescence map of 20 mg UiO-66 and 12 mg ZrPDA in a solution containing (A) DI water, (B) 0.005, (C) 0.010, (D) 0.015, (E) 0.020, (F) 0.025, (G) 0.035 and (H) 0.050 molar $Ni(NO_3)_2$
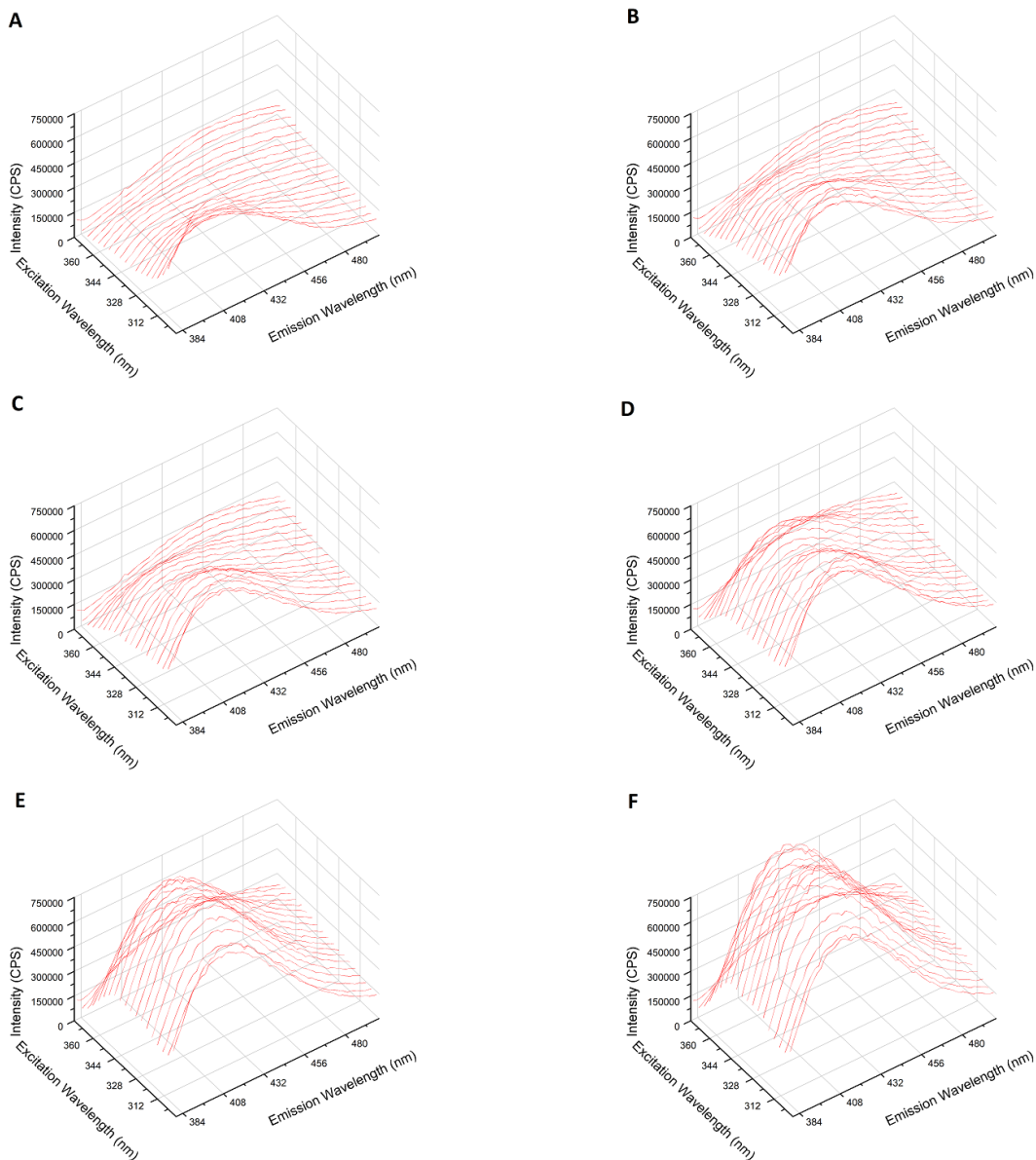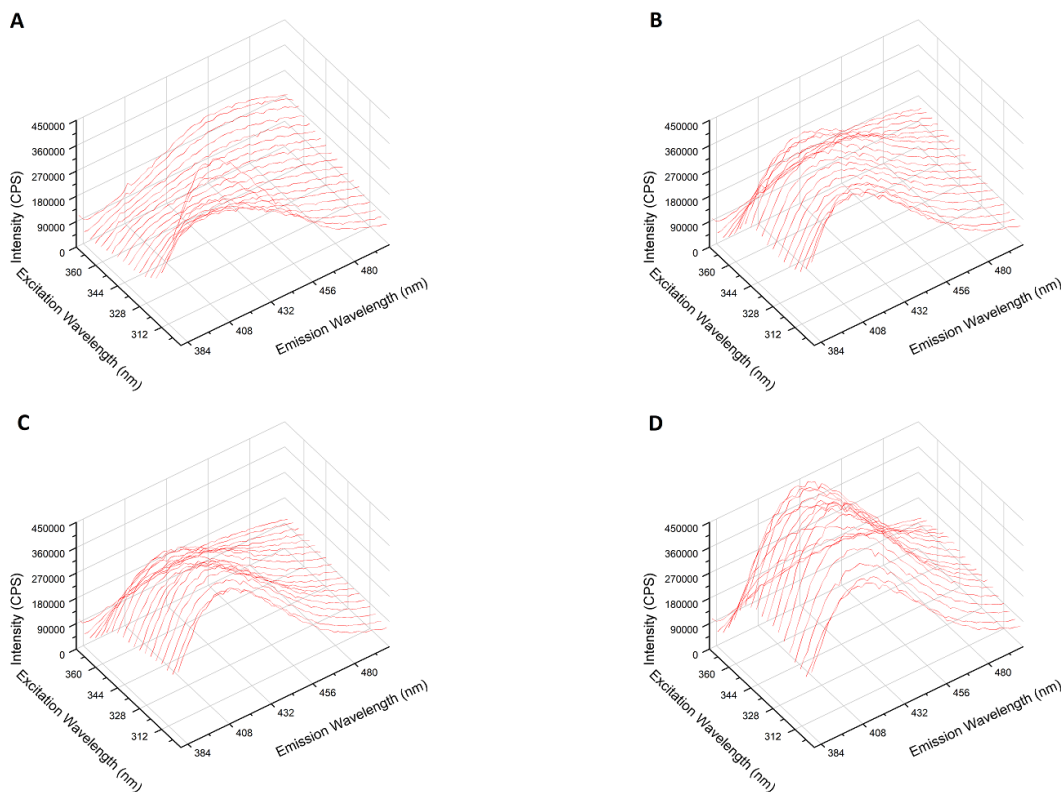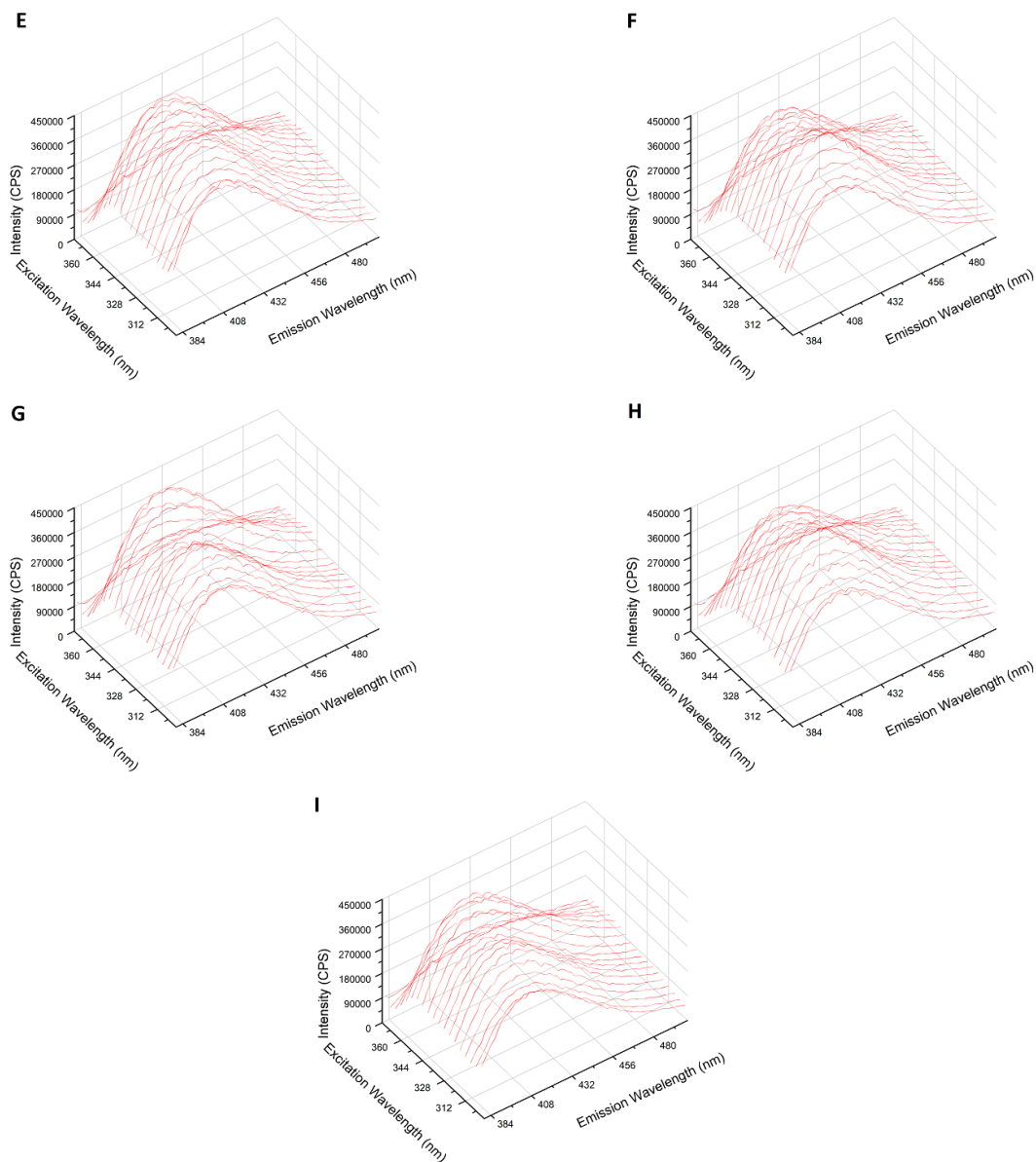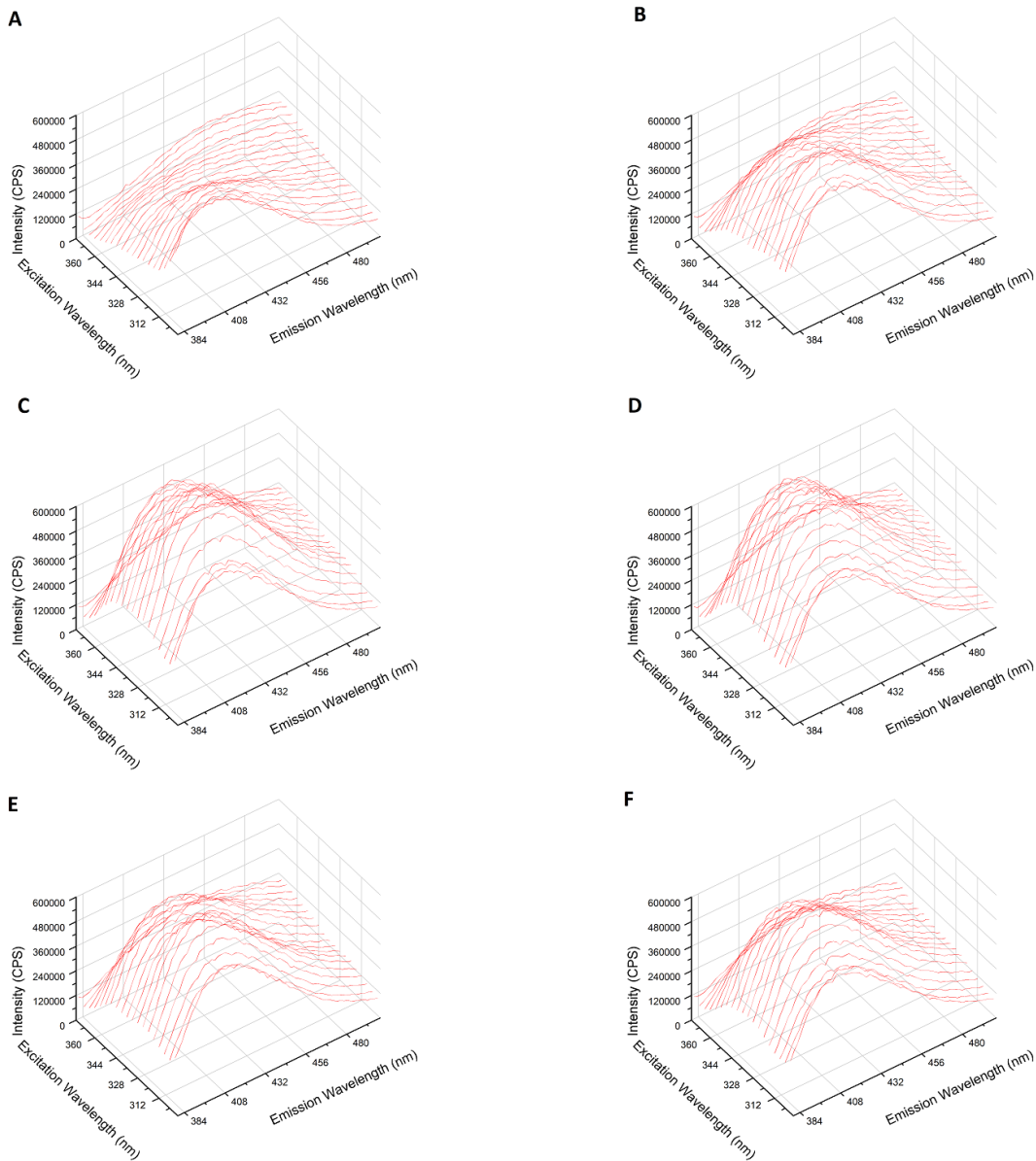
Figure 2.22: 3D luminescence map of 20 mg UiO-66 and 12 mg ZrPDA in a solution containing (A) DI water, (B) 0.005, (C) 0.010, (D) 0.015, (E) 0.020 and (F) 0.025 $Pb(NO_3)_2$

Chapter 3

SUMMARY, CONCLUSION AND FUTURE WORKS

3D luminescence response of UiO-66, UiO-66-NH$_2$ and ZrPDA in solutions containing Pb^{2+}, Ni^{2+}, Ba^{2+} and Cu^{2+} was studied. Also, luminescence response of a UiO-66 and ZrPDA MOF mixture in solutions containing Pb^{2+}, Ni^{2+}, Ba^{2+} and Cu^{2+} was studied.

Table 3.1 summarizes the responses from each MOF to introduction of metal ions. Using this short table makes it easier to compare the response from each MOF. It is also possible to create a similar table comparing the response of a single MOF to introduction of different ions, which can be used as a reference when studying the luminescence in an unknown solution to determine the metal ion and concentration.

Where Table 3.1 has some limitations, it is possible to use Table 3.2. Using Table 3.2, it is possible to study the change in the new peak located at (320,410 nm). In cases like Barium where a large enhancing effect is observed, this new peak can be used to detect even lower concentrations of metal ion than UiO-66 or ZrPDA. Table 3.2 and 3.1 also show the observed peak shift with increasing concentrations of metal ions.

Since all of the systems containing MOF mixture show a similar peak, located at the same position, that shows the same enhancing until 0.01 molar metal ion, it is proposed that there is a new luminescence mode activating at (320,410 nm), which requires a minimum amount of metal ions to be activated.

Table 3.1:

Summary of Luminescence Responses in Single MOF systems

Ion	MOF	Excitation(nm)	Emission(nm)	Response
Pb	UiO-66	300	400	Evanescence quench
	UiO-66-NH$_2$	380→352	452	Enhancing, followed by evanescence quenching
	ZrPDA	372	458	Negligible
Ni	UiO-66	300	390 → 400	Strong initial quench followed by a evanescence quenching
	UiO-66-NH$_2$	378 → 352	456 → 450	Linear enhancing
	ZrPDA	372	458	Small amount of quenching
Cu	UiO-66	300	400	Strong initial quench, followed by quench until peak removal
	UiO-66-NH$_2$	374→ 388	453→ 448	Quenching until peak removal
	ZrPDA	368	450	Quenching
Ba	UiO-66	300	400	Strong initial quench followed by a evanescence quenching
	UiO-66-NH$_2$	356 → 348	444	linear like enhancing
	Zrdpa	368	455	little quenching

Table 3.2:

Summary of Luminescence Responses in UiO-66+ZrPDA system

Ion	Point of Interest	Excitation(nm)	Emission(nm)	Response
Pb	UiO-66 Peak	300	400	Negligible
	New Peak 1	320	410	Enhancing, followed by evanescence quenching
	ZrPDA Peak	368	456	Small evanescence enhance
Ni	UiO-66 Peak	300	$400 \rightarrow 410$	Negligible
	New Peak	320	$418 \rightarrow 410$	Strong initial enhance, followed by evanescence enhance
	ZrPDA Peak	368	458	Small amount of evanescence quench
Cu	UiO-66 Peak	300	$400 \rightarrow 410$	Evanescence quench
	New Peak 1	320	410	Enhancing, followed by evanescence quenching
	New Peak 2	344	410	Enhancing, followed by evanescence quenching
	ZrPDA Peak	368	458	Evanescence quench
Ba	UiO-66 Peak	300	$400 \rightarrow 410$	Enhance
	ZrPDA Peak	$356 \rightarrow 348$	444	linear like enhancing
	New Peak 1	320	$416 \rightarrow 410$	Strong enhance

For future works, the first required step is to study the luminescence mechanism and luminescence mode of ZrPDA. Better understanding of the source of luminescence in ZrPDA provides much needed information in examining its response to addition of metal ions.

For MOF mixture, the source of the new peak must be determined. Also, there needs to be research on the activation mechanism for the new peaks. If they can only be activated by 2+ metal ions, this provides a unique opportunity for distinguishing between different ions, or to keep track of the oxidation level of multivalent metal ions.

Finally, other MOF mixture systems need to be studied. Every day, new MOFs with strong luminescence properties and stability are synthesized. Creating a mixture from varying MOFs can lead to exciting possibilities and open the door to new applications.

REFERENCES

Allendorf, M. D., C. A. Bauer, R. K. Bhakta and R. J. T. Houk, "Luminescent metalorganic frameworks", Chemical Society Reviews **38**, 5, 1330, URL `http://xlink.rsc.org/?DOI=b802352m` (2009).

Armstrong, M. R., S. Senthilnathan, C. J. Balzer, B. Shan, L. Chen and B. Mu, "Particle size studies to reveal crystallization mechanisms of the metal organic framework HKUST-1 during sonochemical synthesis", Ultrasonics Sonochemistry **34**, 365–370 (2017).

Balzer, C. J., M. R. Armstrong, B. Shan and B. Mu, "Composite MOF mixture as volatile organic compound sensor A new approach to LMOF sensors", Materials Letters **190**, 33–36, URL `https://www.sciencedirect.com/science/article/pii/S0167577X16319954` (2017).

Braverman, M. A. and R. L. LaDuca, "Luminescent Two- and Three-Dimensional Zinc Coordination Polymers Containing Isomers of Phenylenediacetate and a Kinked Tethering Organodiimine", Crystal Growth & Design **7**, 11, 2343–2351, URL `http://pubs.acs.org/doi/abs/10.1021/cg070599f` (2007).

Cavka, J. H., S. Jakobsen, U. Olsbye, N. Guillou, C. Lamberti, S. Bordiga and K. P. Lillerud, "A New Zirconium Inorganic Building Brick Forming Metal Organic Frameworks with Exceptional Stability", Journal of the American Chemical Society **130**, 42, 13850–13851, URL `http://pubs.acs.org/doi/abs/10.1021/ja8057953` (2008).

Chavan, S., J. G. Vitillo, D. Gianolio, O. Zavorotynska, B. Civalleri, S. Jakobsen, M. H. Nilsen, L. Valenzano, C. Lamberti, K. P. Lillerud and S. Bordiga, "H2 storage in isostructural UiO-67 and UiO-66 MOFs", Phys. Chem. Chem. Phys. **14**, 5, 1614–1626, URL `http://xlink.rsc.org/?DOI=C1CP23434J` (2012).

Chen, B., L. Wang, F. Zapata, G. Qian and E. B. Lobkovsky, "A Luminescent Microporous MetalOrganic Framework for the Recognition and Sensing of Anions", Journal of the American Chemical Society **130**, 21, 6718–6719, URL `http://pubs.acs.org/doi/abs/10.1021/ja802035e` (2008).

Chen, B., Y. Yang, F. Zapata, G. Lin, G. Qian and E. Lobkovsky, "Luminescent Open Metal Sites within a MetalOrganic Framework for Sensing Small Molecules", Advanced Materials **19**, 13, 1693–1696, URL `http://doi.wiley.com/10.1002/adma.200601838` (2007).

Cui, Y., Y. Yue, G. Qian and B. Chen, "Luminescent Functional MetalOrganic Frameworks", Chemical Reviews **112**, 2, 1126–1162, URL `http://pubs.acs.org/doi/10.1021/cr200101d` (2012).

Fang, Q., G. Zhu, M. Xue, J. Sun, F. Sun and S. Qiu, "Structure, Luminescence, and Adsorption Properties of Two Chiral Microporous MetalOrganic Frameworks", Inorganic Chemistry **45**, 9, 3582–3587, URL `http://dx.doi.org/10.1021/ic051810k` (2006).

Flage-Larsen, E. and K. Thorshaug, "Linker Conformation Effects on the Band Gap in MetalOrganic Frameworks", Inorganic Chemistry **53**, 5, 2569–2572, URL `http://pubs.acs.org/doi/10.1021/ic4028628` (2014).

Kandiah, M., M. H. Nilsen, S. Usseglio, S. Jakobsen, U. Olsbye, M. Tilset, C. Larabi, E. A. Quadrelli, F. Bonino and K. P. Lillerud, "Synthesis and Stability of Tagged UiO-66 Zr-MOFs", Chemistry of Materials **22**, 24, 6632–6640, URL `http://pubs.acs.org/doi/abs/10.1021/cm102601v` (2010a).

Kandiah, M., S. Usseglio, S. Svelle, U. Olsbye, K. P. Lillerud and M. Tilset, "Postsynthetic modification of the metal-organic framework compound UiO-66", J. Mater. Chem. **20**, 44, 9848–9851, URL `http://dx.doi.org/10.1039/C0JM02416C` (2010b).

Kim, T. K., J. H. Lee, D. Moon and H. R. Moon, "Luminescent Li-Based MetalOrganic Framework Tailored for the Selective Detection of Explosive Nitroaromatic Compounds: Direct Observation of Interaction Sites", Inorganic Chemistry **52**, 2, 589–595, URL `http://pubs.acs.org/doi/10.1021/ic3011458` (2013).

Li, M.-X., H. Wang, S.-W. Liang, M. Shao, X. He, Z.-X. Wang and S.-R. Zhu, "Solvothermal Synthesis and Diverse Coordinate Structures of a Series of Luminescent Copper(I) Thiocyanate Coordination Polymers Based on N-Heterocyclic Ligands", Crystal Growth & Design **9**, 11, 4626–4633, URL `http://pubs.acs.org/doi/abs/10.1021/cg900079p` (2009).

Lin, C.-K., D. Zhao, W.-Y. Gao, Z. Yang, J. Ye, T. Xu, Q. Ge, S. Ma and D.-J. Liu, "Tunability of Band Gaps in MetalOrganic Frameworks", Inorganic Chemistry **51**, 16, 9039–9044, URL `http://pubs.acs.org/doi/10.1021/ic301189m` (2012).

Liu, T., J. Lü, L. Shi, Z. Guo and R. Cao, "Conformation control of a flexible 1,4-phenylenediacetate ligand in coordination complexes: a rigidity-modulated strategy", CrystEngComm **11**, 4, 583–588, URL `http://xlink.rsc.org/?DOI=B813444H` (2009).

Luo, F. and S. R. Batten, "Metalorganic framework (MOF): lanthanide(iii)-doped approach for luminescence modulation and luminescent sensing", Dalton Transactions **39**, 19, 4485, URL `http://xlink.rsc.org/?DOI=c002822n` (2010).

Mu, B. and B. Shan, "Phototunable metal-organic framework compositions, and methods of synthesis thereof", URL `https://www.google.com/patents/US9716239` (2017).

Murray, L. J., M. Dinc and J. R. Long, "Hydrogen storage in metalorganic frameworks", Chemical Society Reviews **38**, 5, 1294, URL `http://xlink.rsc.org/?DOI=b802256a` (2009).

Needleman, H., "Lead Poisoning", Annual Review of Medicine **55**, 1, 209–222, URL http://www.annualreviews.org/doi/10.1146/annurev.med.55.091902.103653 (2004).

Rao, X., T. Song, J. Gao, Y. Cui, Y. Yang, C. Wu, B. Chen and G. Qian, "A Highly Sensitive Mixed Lanthanide MetalOrganic Framework Self-Calibrated Luminescent Thermometer", Journal of the American Chemical Society **135**, 41, 15559–15564, URL http://pubs.acs.org/doi/10.1021/ja407219k (2013).

Sampson, R. J. and A. S. Winter, "THE RACIAL ECOLOGY OF LEAD POISON-ING", Du Bois Review: Social Science Research on Race **13**, 02, 261–283, URL http://www.journals.cambridge.org/abstract_S1742058X16000151 (2016).

Shustova, N. B., A. F. Cozzolino, S. Reineke, M. Baldo and M. Dinc, "Selective Turn-On Ammonia Sensing Enabled by High-Temperature Fluorescence in MetalOrganic Frameworks with Open Metal Sites", Journal of the American Chemical Society **135**, 36, 13326–13329, URL http://pubs.acs.org/doi/10.1021/ja407778a (2013).

Song, Z., F. Qiu, E. W. Zaia, Z. Wang, M. Kunz, J. Guo, M. Brady, B. Mi and J. J. Urban, "Dual-Channel, Molecular-Sieving Core/Shell ZIF@MOF Architectures as Engineered Fillers in Hybrid Membranes for Highly Selective CO_2 Separation", Nano Letters **17**, 11, 6752–6758, URL http://pubs.acs.org/doi/10.1021/acs.nanolett.7b02910 (2017).

Wang, G.-H., Z.-G. Li, H.-Q. Jia, N.-H. Hu and J.-W. Xu, "Metalorganic frameworks based on the pyridine-2,3-dicarboxylate and a flexible bispyridyl ligand: syntheses, structures, and photoluminescence", CrystEngComm **11**, 2, 292–297, URL http://xlink.rsc.org/?DOI=B809557D (2009).

Weber, I. T., A. J. G. de Melo, M. A. d. M. Lucena, M. O. Rodrigues and S. Alves Junior, "High Photoluminescent MetalOrganic Frameworks as Optical Markers for the Identification of Gunshot Residues", Analytical Chemistry **83**, 12, 4720–4723, URL http://pubs.acs.org/doi/abs/10.1021/ac200680a (2011).

Wei Chen, ., . Jia-Yu Wang, . Cheng Chen, . Qi Yue, . Hong-Ming Yuan, , . Jie-Sheng Chen, * and S.-N. Wang, "Photoluminescent MetalOrganic Polymer Constructed from Trimetallic Clusters and Mixed Carboxylates", URL http://pubs.acs.org/doi/abs/10.1021/ic025871j (2003).

Xiao, Y., Y. Cui, Q. Zheng, S. Xiang, G. Qian and B. Chen, "A microporous luminescent metalorganic framework for highly selective and sensitive sensing of Cu2+ in aqueous solution", Chemical Communications **46**, 30, 5503, URL http://xlink.rsc.org/?DOI=c0cc00148a (2010).

Yang, G.-P., Y.-Y. Wang, W.-H. Zhang, A.-Y. Fu, R.-T. Liu, E. K. Lermontova and Q.-Z. Shi, "A series of Zn(ii) coordination complexes derived from isomeric phenylenediacetic acid and dipyridyl ligands: syntheses, crystal structures, and characterizations", CrystEngComm **12**, 5, 1509, URL http://xlink.rsc.org/?DOI=b915889h (2010).

Zhang, K.-L., H.-Y. Gao, Z.-C. Pan, W. Liang and G.-W. Diao, "Preparation and characterization of two three-dimensional metalorganic photoluminescent supramolecular networks", Polyhedron **26**, 17, 5177–5184, URL `http://www.sciencedirect.com/science/article/pii/S0277538707004500` (2007).